

Oxide MBE— A Tool to Create Artificial Quantum Materials

Darrell G. Schlom

*Department of Materials Science and Engineering
Cornell University*

Kavli Institute at Cornell for Nanoscale Science

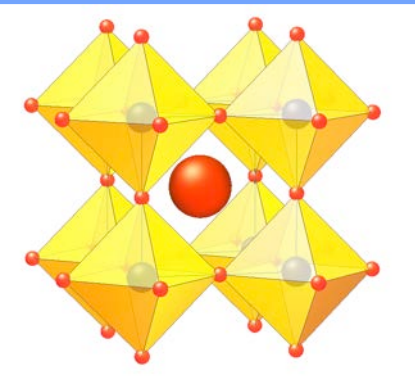
Outline

- What is MBE and what is it good for?
Greatest hits of MBE
- How to grow your favorite oxide quantum material by MBE?
Nuts and bolts of oxide MBE
- Oxide MBE growth of quantum materials
Case studies—including Sr_2RuO_4
- How can I gain access to an oxide MBE if I don't have one?
Use PARADIM's oxide MBE (+ ARPES + ...)

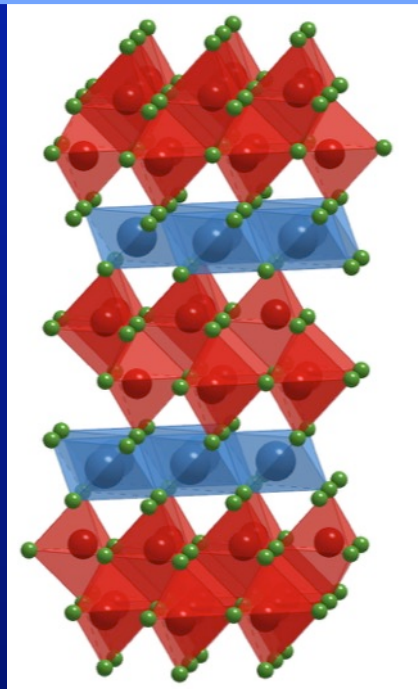
Nuts and Bolts of Oxide MBE

- Mean Free Path (maximum P_{O_2})
- Minimum P_{O_2} , need for P_{O_3} , Optimal T_{sub}
- MBE System, Sources, and Crucibles
- **Composition Control**
 - Adsorption-Controlled Growth
 - Flux-Controlled Growth
- **Substrates**

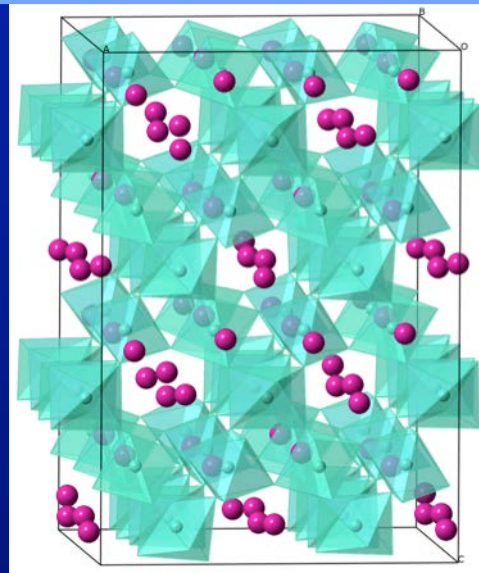
Wacky Oxides we Grow



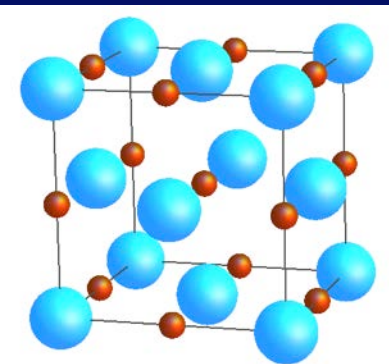
PbTiO_3
or
 BiFeO_3
or
 BiMnO_3



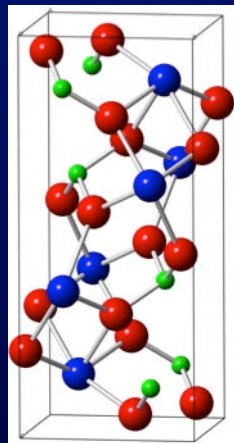
LuFe_2O_4




$\alpha\text{-Bi}_2\text{Sn}_2\text{O}_7$
(352 atoms/unit cell)
or
 $\text{Bi}_2\text{Ru}_2\text{O}_7$

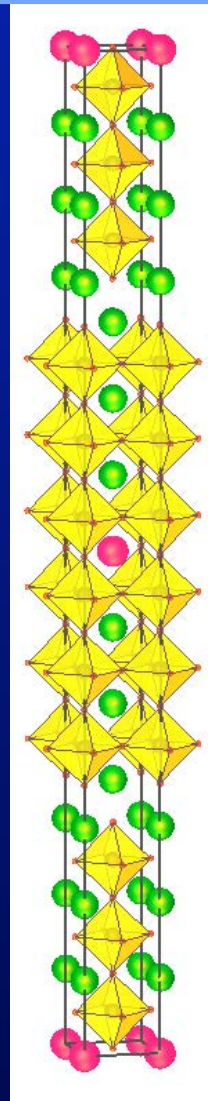


EuO



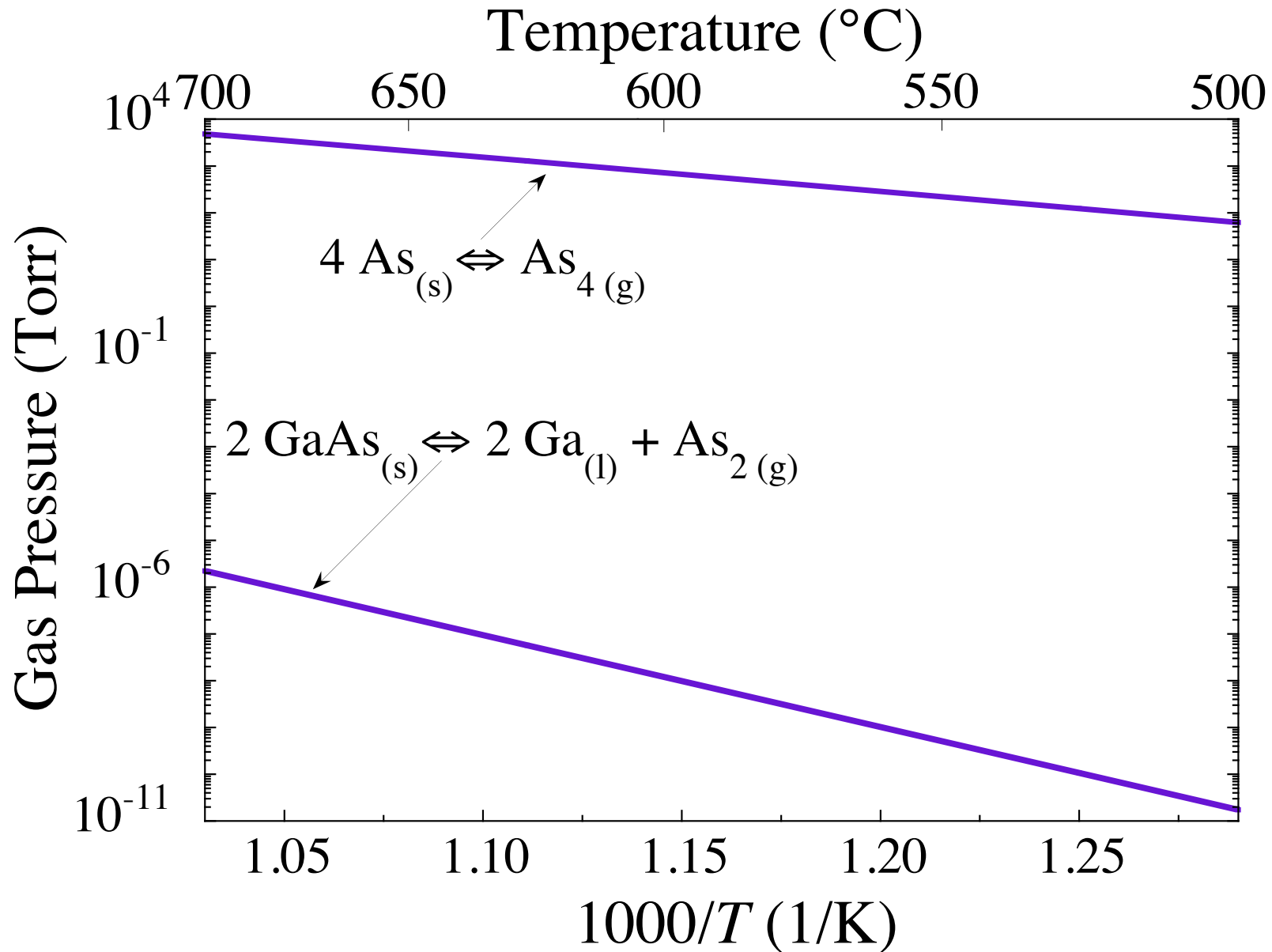
BiVO_4

 The image cannot be displayed. Your computer may not have enough memory to open the image, or the image may have been corrupted. Restart your computer, and then open the file again. If the red x still appears, you may have to delete the image and then insert it again.



$\text{Sr}_7\text{Ti}_6\text{O}_{19}$ $\text{BaSr}_6\text{Ti}_6\text{O}_{19}$

Adsorption-Controlled Growth of GaAs



C.D. Theis, J. Yeh, D.G. Schlom, M.E. Hawley, and G.W. Brown,

“Adsorption-Controlled Growth of PbTiO_3 by Reactive Molecular Beam Epitaxy,” *Thin Solid Films* **325** (1998) 107-114.

Adsorption-Controlled Growth of

- **Plumbites**

- **PbTiO₃** — C.D. Theis *et al.*, *J. Cryst. Growth* **174** (1997) 473-479.
- **PbZrO₃** — (unpublished)

- **Bismuthates**

- **Bi₂Sr₂CuO₆** — S. Migita *et al.*, *Appl. Phys. Lett.* **71** (1997) 3712-3714.
- **Bi₄Ti₃O₁₂** — C.D. Theis *et al.*, *Appl. Phys. Lett.* **72** (1998) 2817-2819.
- **BiFeO₃** — J.F. Ihlefeld *et al.*, *Appl. Phys. Lett.* **91** (2007) 071922.
- **BiMnO₃** — J.H. Lee *et al.*, *Appl. Phys. Lett.* **96** (2010) 262905.
- **BiVO₄** — S. Stoughton *et al.*, *APL Materials* **1** (2013) 042112.
- **Bi₂Sn₂O₇** and **Bi₂Ru₂O₇** — (unpublished)

- **Titanates by MOMBE**

- **SrTiO₃** — B. Jalan *et al.*, *Appl. Phys. Lett.* **95** (2009) 032906.
- **GdTiO₃** — P. Moetakef *et al.*, *J. Vac. Sci. Technol. A* **31** (2013) 041503.
- **BaTiO₃** — Y. Matsubara *et al.*, *Appl. Phys. Express* **7** (2014) 125502.
- **CaTiO₃** — R.C. Haislmaier *et al.*, *Adv. Funct. Mater.* **26** (2016) 7271.

Adsorption-Controlled Growth of

- **Ferrites**

- **LuFe₂O₄** — C.M. Brooks *et al.*, *Appl. Phys. Lett.* **101** (2012) 132907.

- **Vanadates by MOMBE**

- **LaVO₃** — H.-T. Zhang *et al.*, *Appl. Phys. Lett.* **106** (2015) 233102.

- **(La,Sr)VO₃** — M. Brahlek *et al.*, *Appl. Phys. Lett.* **109** (2016) 101903.

- **Ruthenates**

- **SrRuO₃** — D.E. Shai *et al.*, *Phys. Rev. Lett.* **110** (2013) 087004.

- **Sr₂RuO₄** and **Ba₂RuO₄** — B. Burganov *et al.*, *Phys. Rev. Lett.* **116** (2016) 197003.

- **CaRuO₃** — H.P. Nair *et al.*, *APL Mater.* **6** (2018) 046101.

- **Ca₂RuO₄** — (unpublished)

Adsorption-Controlled Growth of

- **Iridates**

- **Ba₂IrO₄** — M. Uchida *et al.*, *Phys. Rev. B* **90** (2014) 075142.

- **SrIrO₃** and **Sr₂IrO₄** — Y.F. Nie *et al.*, *Phys. Rev. Lett.* **114** (2015) 016401.

- **Stannates by MOCVD**

- **BaSnO₃** — A. Prakash *et al.*, *J. Mater. Chem. C* **5** (2017) 5730 .

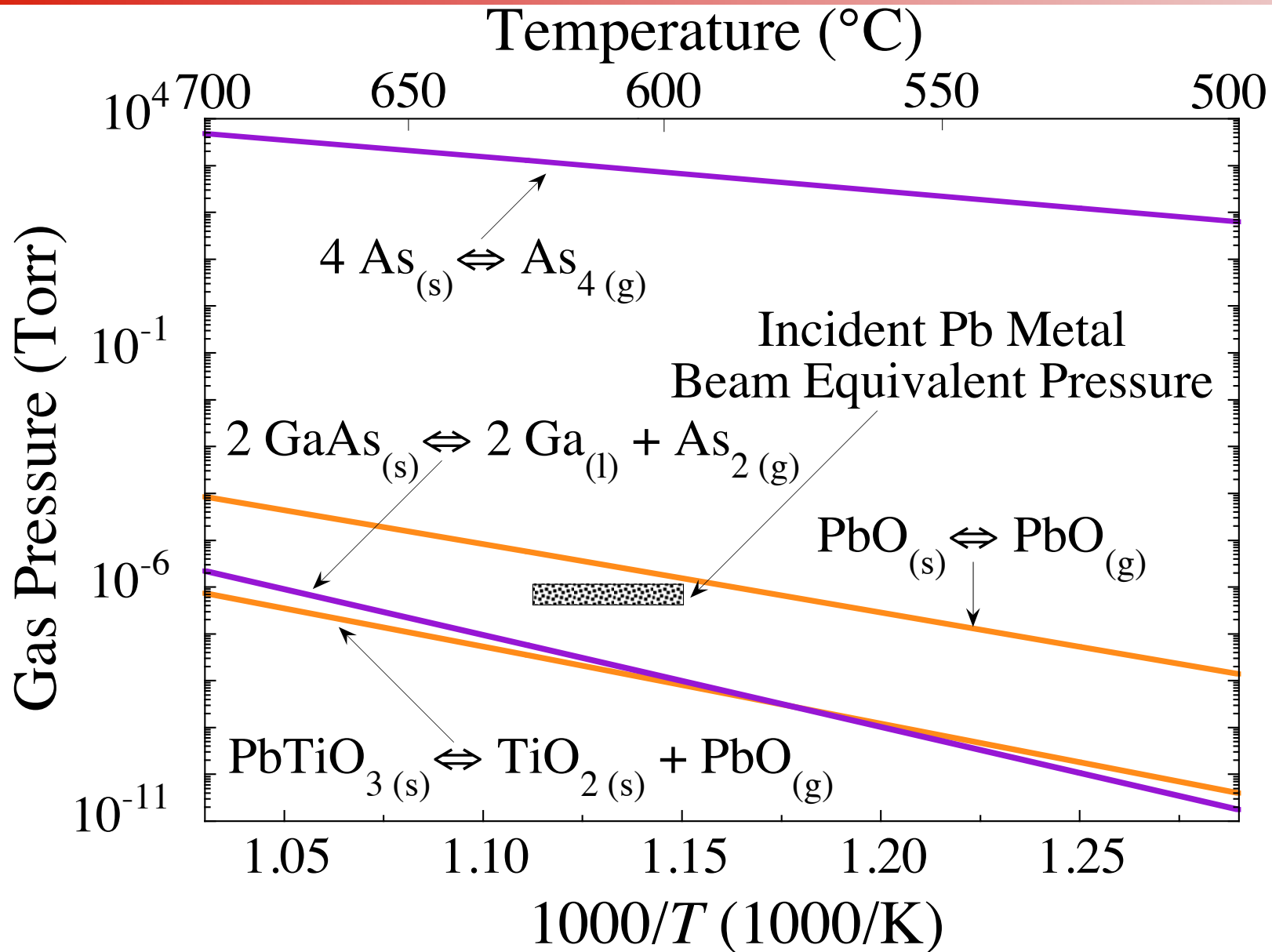
- **Stannates**

- **BaSnO₃** — H. Paik *et al.*, *APL Materials* **5** (2017) 116107.

- **Other**

- **EuO** — R.W. Ulbricht *et al.*, *Appl. Phys. Lett.* **93** (2008) 102105.

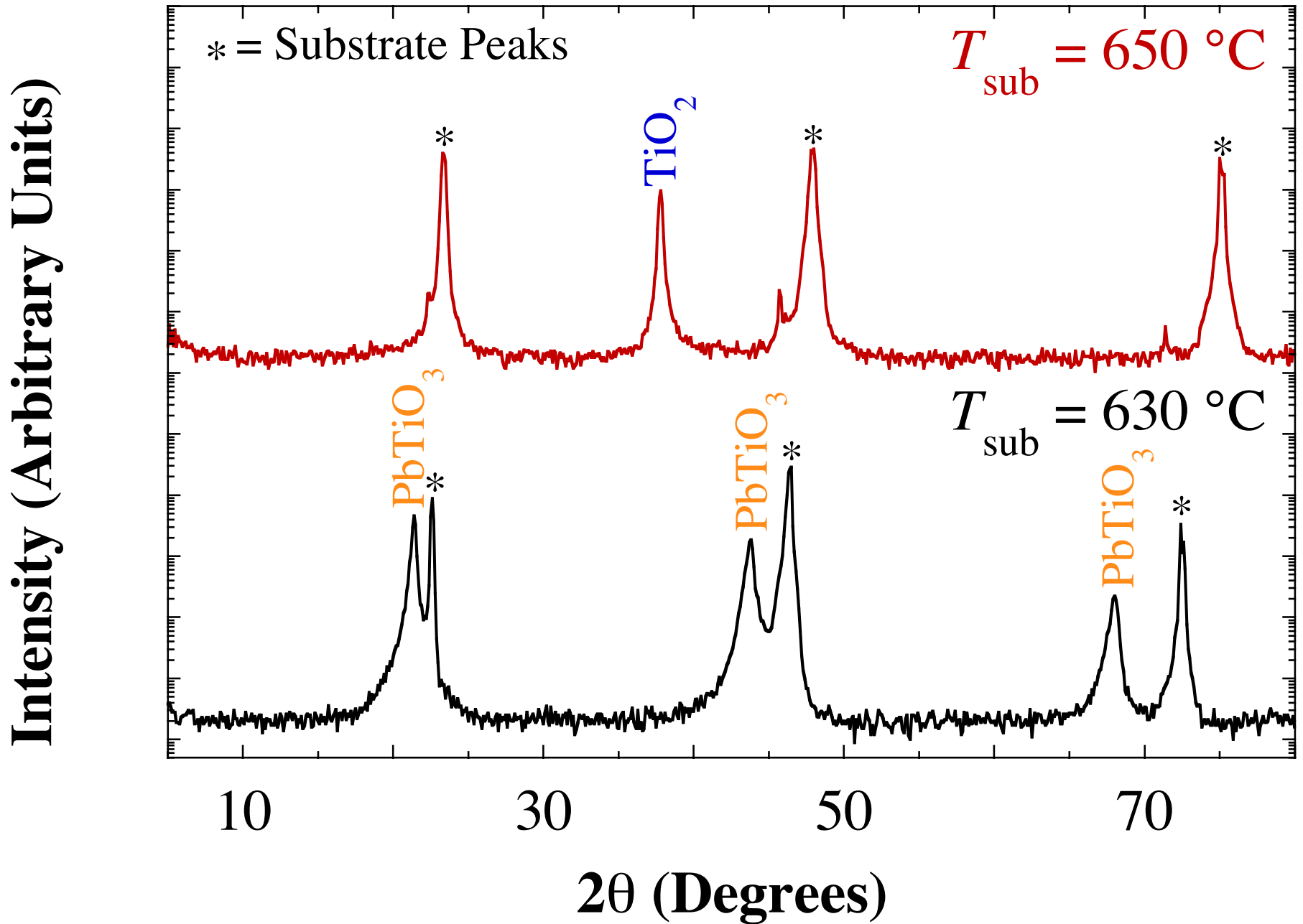
Adsorption-Controlled Growth of PbTiO₃



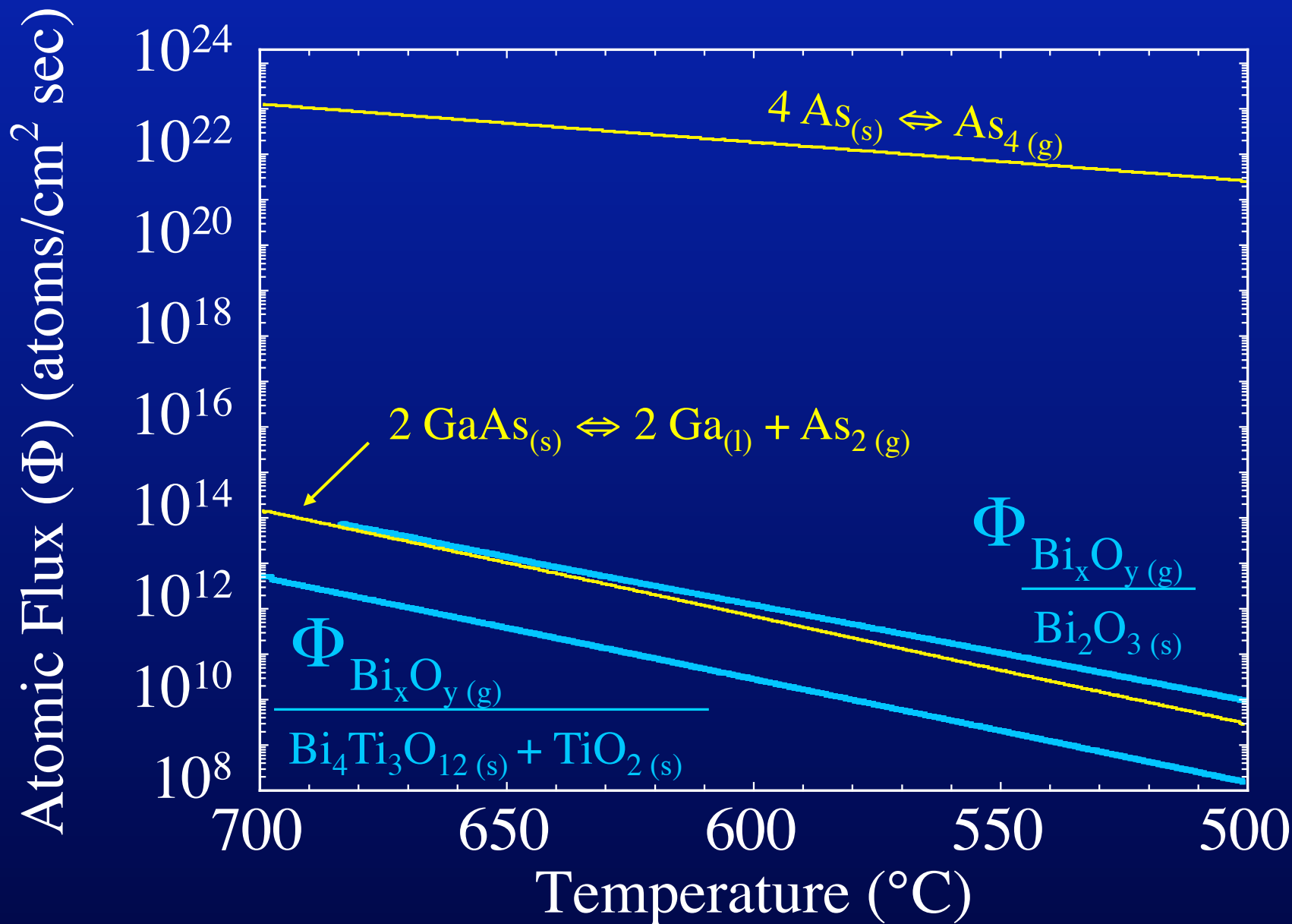
C.D. Theis, J. Yeh, D.G. Schlom, M.E. Hawley, and G.W. Brown,

“Adsorption-Controlled Growth of PbTiO₃ by Reactive Molecular Beam Epitaxy,” *Thin Solid Films* **325** (1998) 107-114.

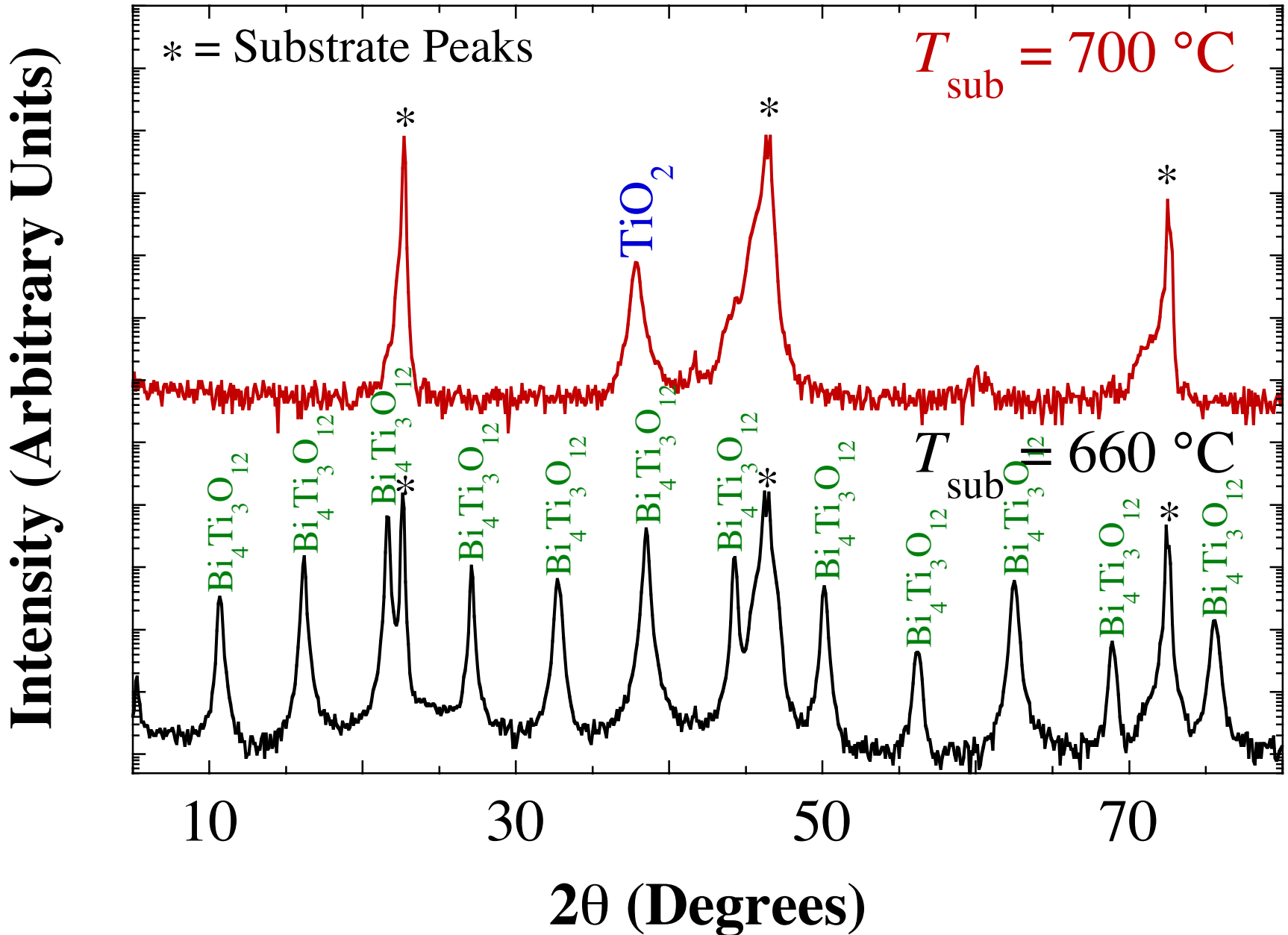
Adsorption-Controlled Growth of PbTiO_3



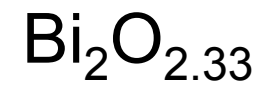
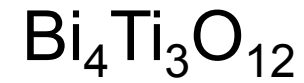
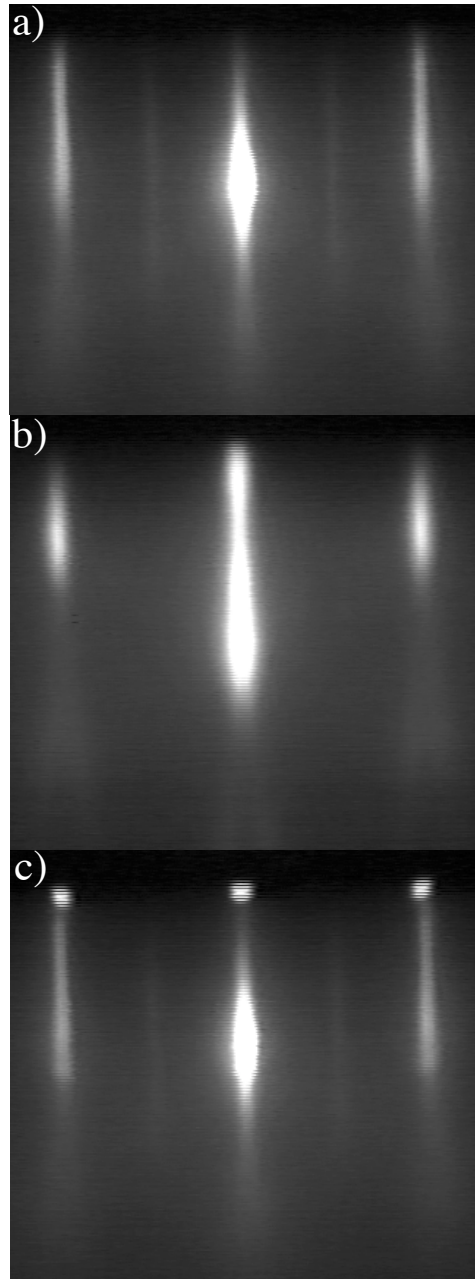
Growth of $\text{Bi}_4\text{Ti}_3\text{O}_{12}$ by MBE



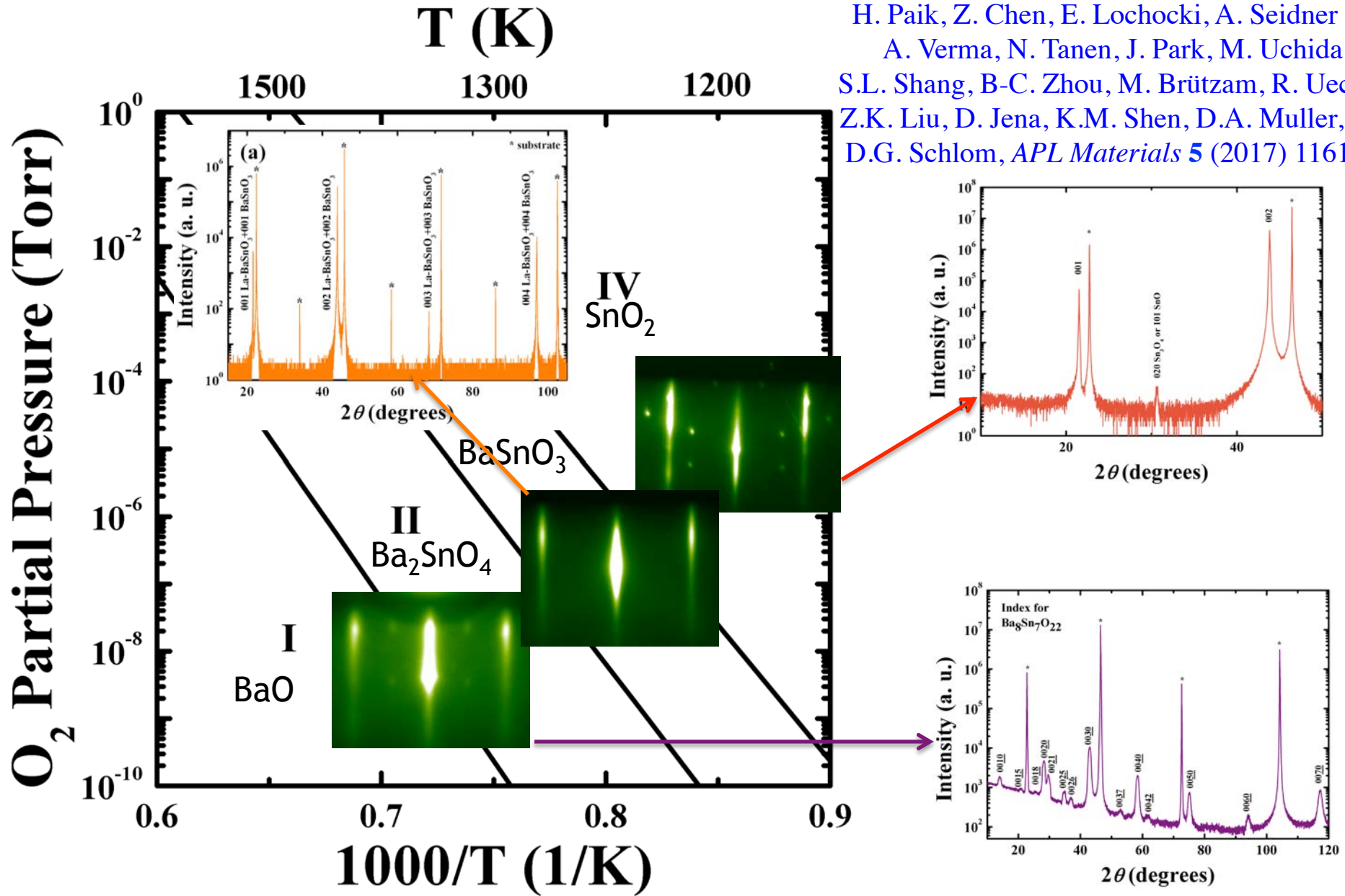
Adsorption-Controlled Growth of $\text{Bi}_4\text{Ti}_3\text{O}_{12}$



Adsorption-Controlled Growth of $\text{Bi}_4\text{Ti}_3\text{O}_{12}$



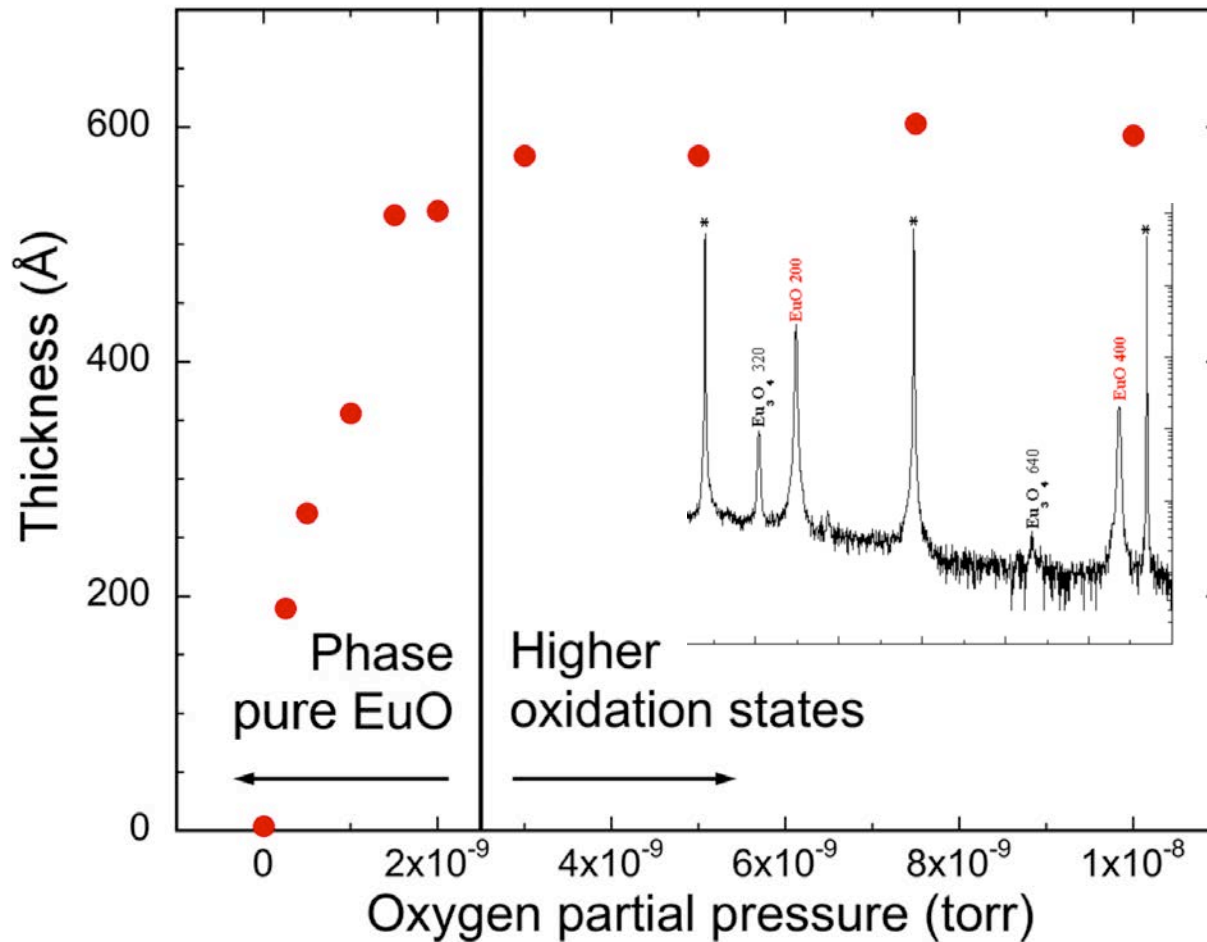
Growth of BaSnO₃ by MBE



H. Paik, Z. Chen, E. Lochocki, A. Seidner H.,
 A. Verma, N. Tanen, J. Park, M. Uchida,
 S.L. Shang, B-C. Zhou, M. Brützm, R. Uecker,
 Z.K. Liu, D. Jena, K.M. Shen, D.A. Muller, and
 D.G. Schlom, *APL Materials* **5** (2017) 116107.

Adsorption-Controlled Growth of EuO

Eu Flux = 1.1×10^{14} Eu atoms/(cm² s), $T_{\text{sub}} = 590$ °C
EuO film thickness (from RBS) after 30 min



YAlO₃ without Eu flux (a)

YAlO₃ with Eu flux (b)

with EuO deposition (c)

Adsorption-Controlled SrTiO₃

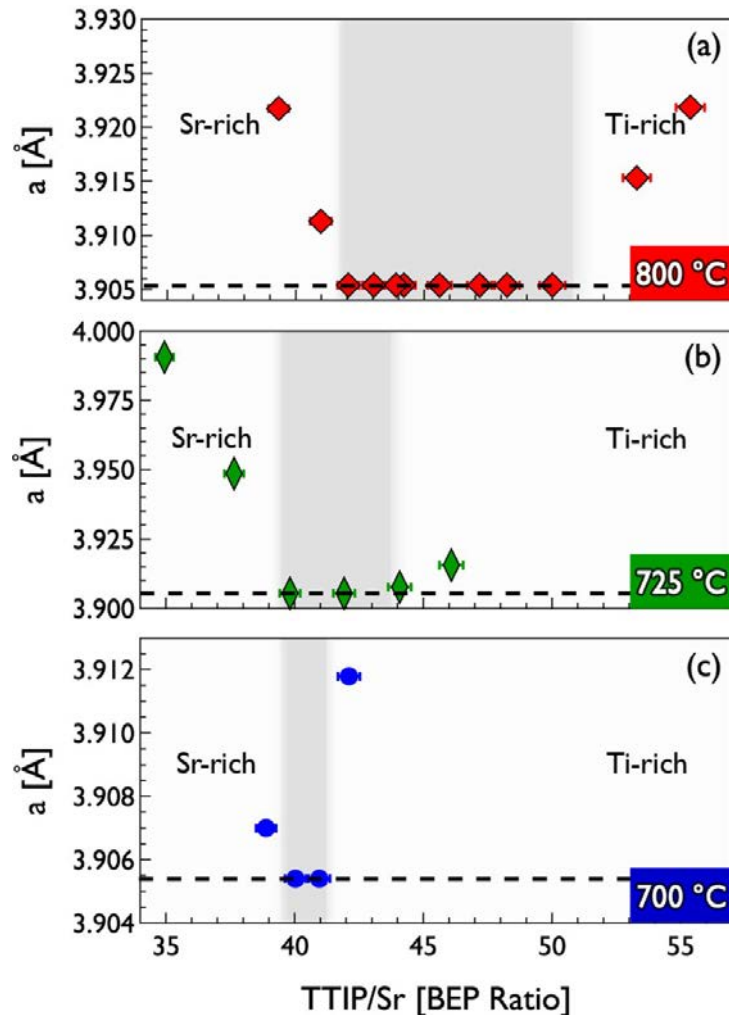


FIG. 3. (Color online) Out-of-plane lattice parameter as a function of TTIP/Sr BEP ratio for epitaxial SrTiO₃ films grown on (001)SrTiO₃ at (a) 800 °C, (b) 725 °C, and (c) 700 °C. All films were grown using an oxygen BEP of 8×10^{-6} torr. The darker gray-shaded region shows the growth window for stoichiometric films with a lattice parameter that is equivalent to that of the substrate at each temperature.

MOMBE Sources

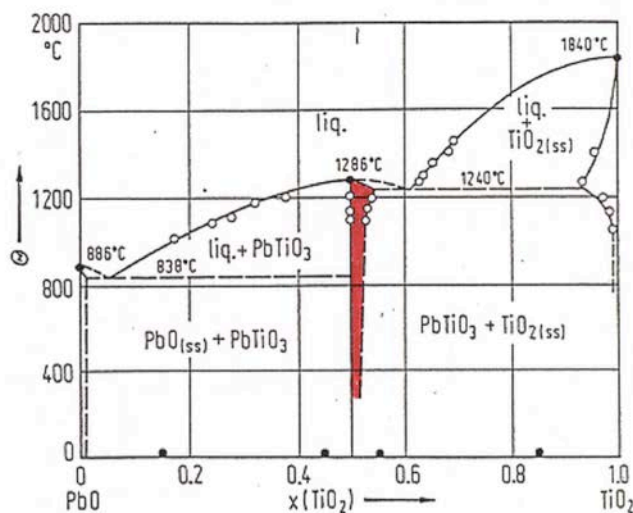
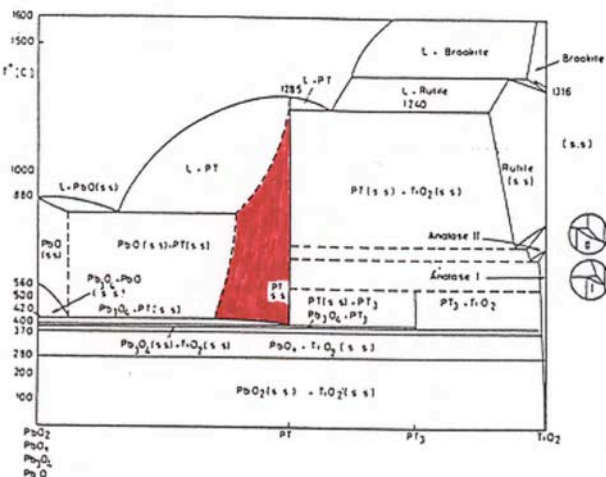
Sr

Ti(OC₃H₇)₄

Oxygen Plasma

B. Jalan, P. Moetakef, and S. Stemmer,
Applied Physics Letters **95** (2009) 032906.

Single-Phase Field of GaAs vs. PbTiO₃



PbTiO₃

Single-phase film does not imply stoichiometric film

GaAs

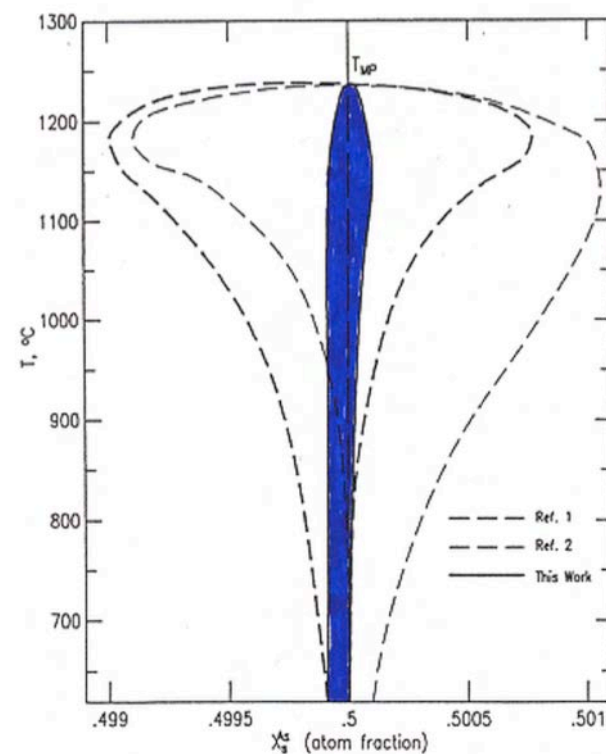


Fig. 8337—GaAs solidus curve. Curves represent the calculated deviations from stoichiometry for solid GaAs. A. I. Ivashchenko, F. Ya. Kopanskaya, and G. S. Kuzmenko, *J. Phys. Chem. Solids*, 45 [8-9] 871-875 (1984).

III-V Phase Diagrams

121301-12 D. T. J. Hurle

J. Appl. Phys. **107**, 121301 (2010)

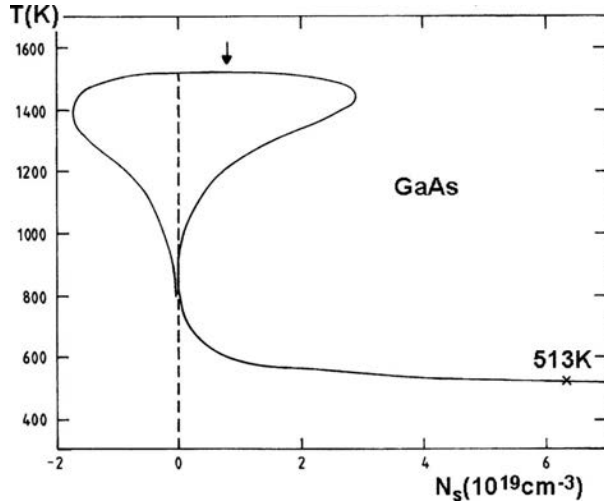


FIG. 2. The calculated solidus of gallium arsenide showing the catastrophic deviation from stoichiometry at low temperature under arsenic-rich conditions. Arrow marks the congruent point.

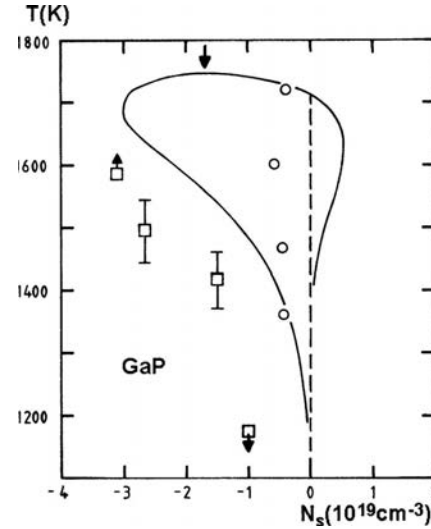


FIG. 3. Calculated GaP solidus. Arrow marks the congruent point. Experimental data: Jordan *et al.* (○); Morozov *et al.* (□).

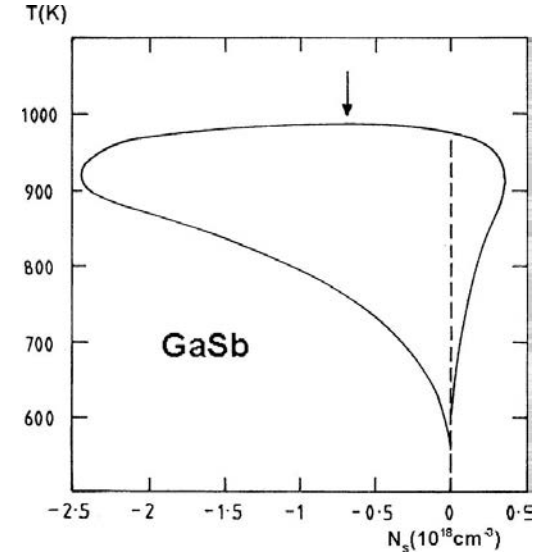


FIG. 5. Calculated GaSb solidus. Arrow marks the congruent point.

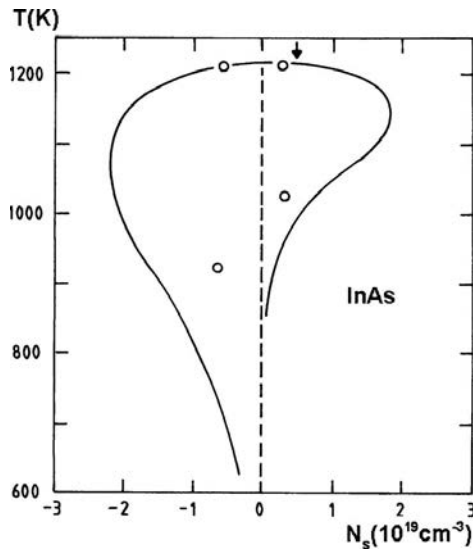


FIG. 7. Calculated InAs solidus. Arrow marks the congruent point. Data points: Bublik *et al.* (○).

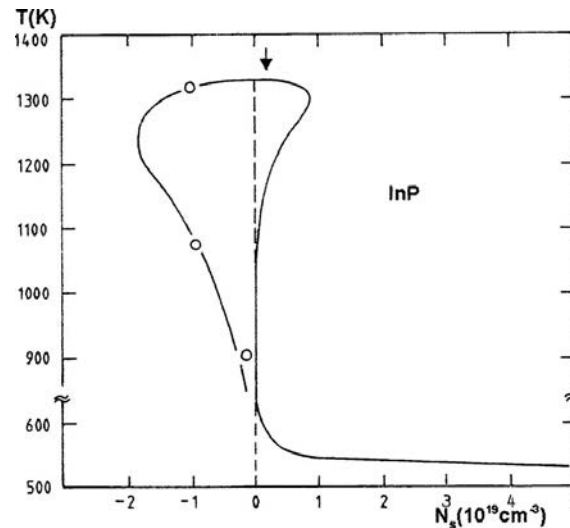


FIG. 8. Calculated InP solidus. Arrow marks the congruent point. Data points: Morozov *et al.* (Ref. 34) (○).

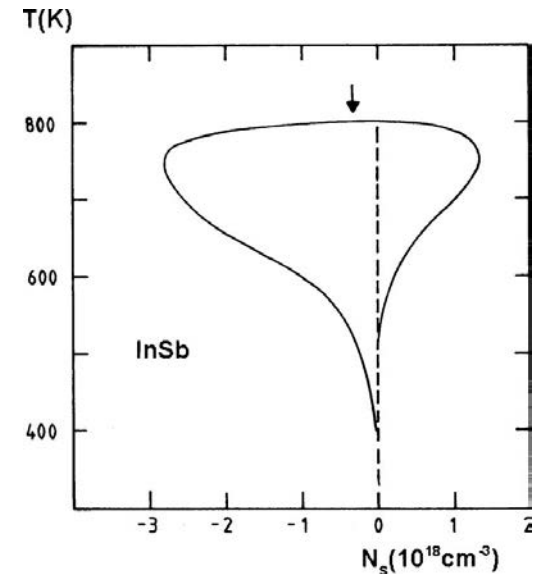
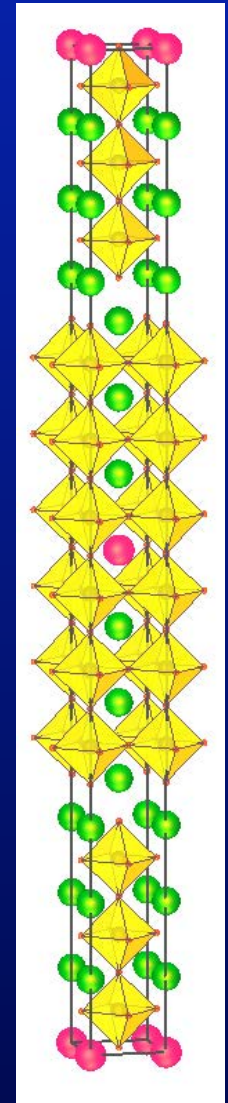
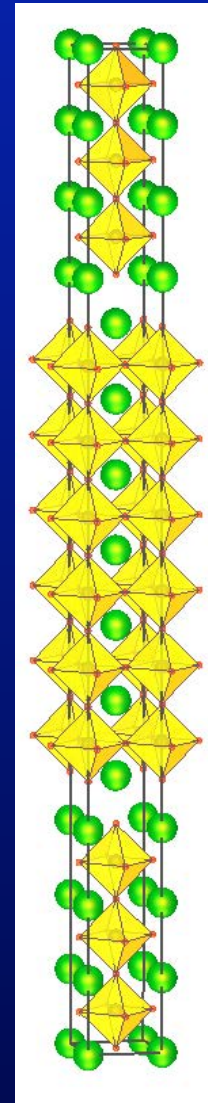


FIG. 9. Calculated InSb solidus. Arrow marks the congruent point.

Challenge

What if the wacky oxide
you desire cannot be
grown by adsorption-
control?



$\text{Sr}_7\text{Ti}_6\text{O}_{19}$ $\text{BaSr}_6\text{Ti}_6\text{O}_{19}$

Nuts and Bolts of Oxide MBE

- Mean Free Path (maximum P_{O_2})
- Minimum P_{O_2} , need for P_{O_3} , Optimal T_{sub}
- MBE System, Sources, and Crucibles
- Composition Control
 - Adsorption-Controlled Growth
 - **Flux-Controlled Growth**
- **Substrates**

Reflection High-Energy Electron Diffraction (RHEED) Oscillations

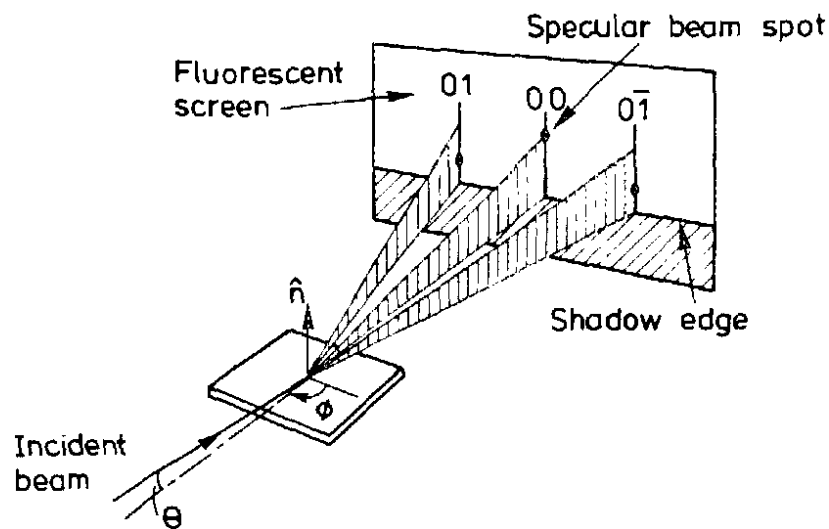
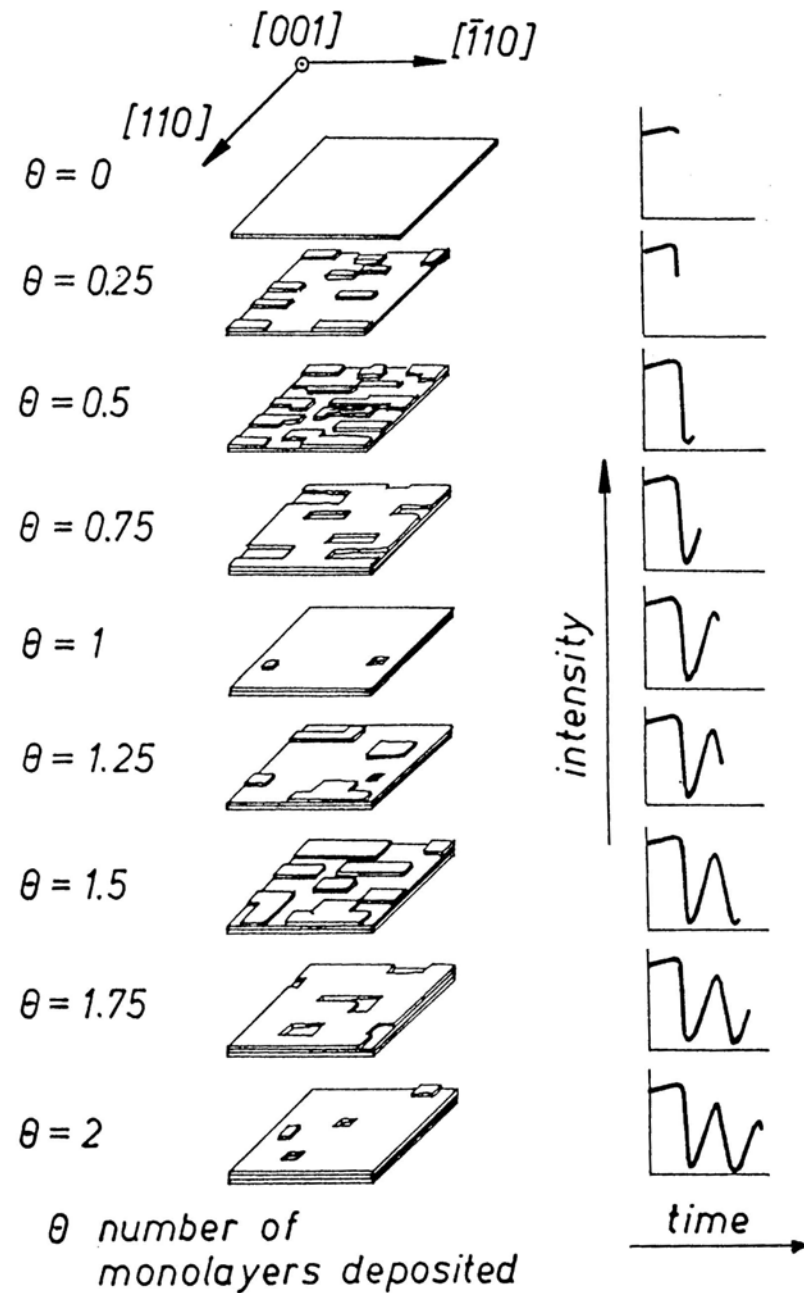


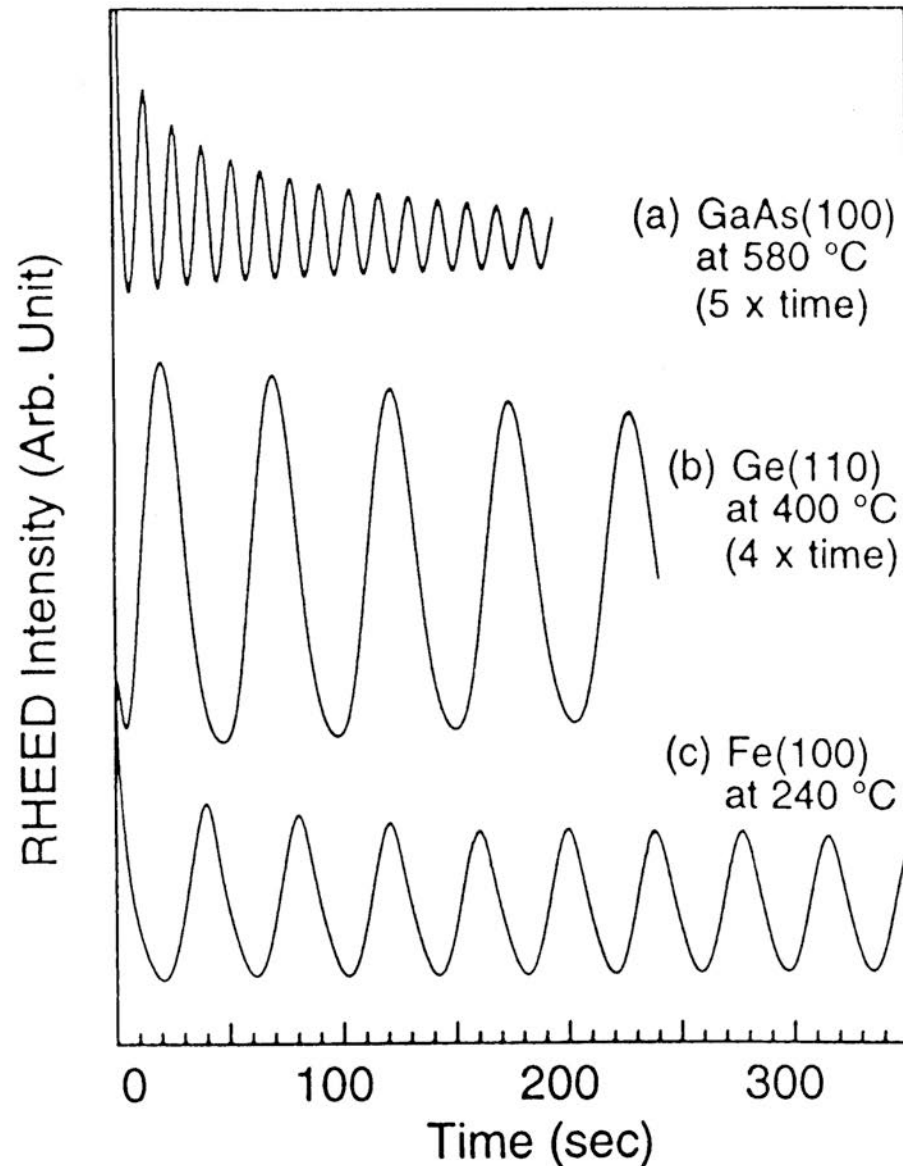
FIG. 1. Schematic diagram of RHEED geometry showing the incident beam at an angle θ to the surface plane; azimuthal angle ϕ . The elongated spots indicate the intersection of the Ewald sphere with the 01 , 00 , and $0\bar{1}$ rods.



B. Bölger and P. K. Larsen, *Review of Scientific Instruments* **57** (1986) 1363-1367.

B.A. Joyce, P.J. Dobson, J.H. Neave, K. Woodbridge, J. Zhang, P.K. Larsen, and B Bölger, *Surface Science* **168** (1986) 423-438.

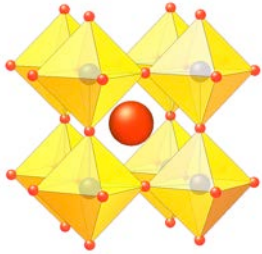
Conventional RHEED Oscillations



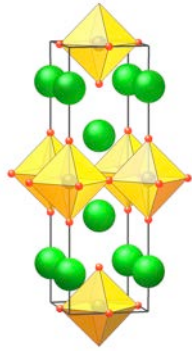
Molecular Beam Epitaxy: *Applications to Key Materials*,
edited by R.F.C. Farrow (Noyes, Park Ridge, 1995), p. 694.

Conventional RHEED Oscillations

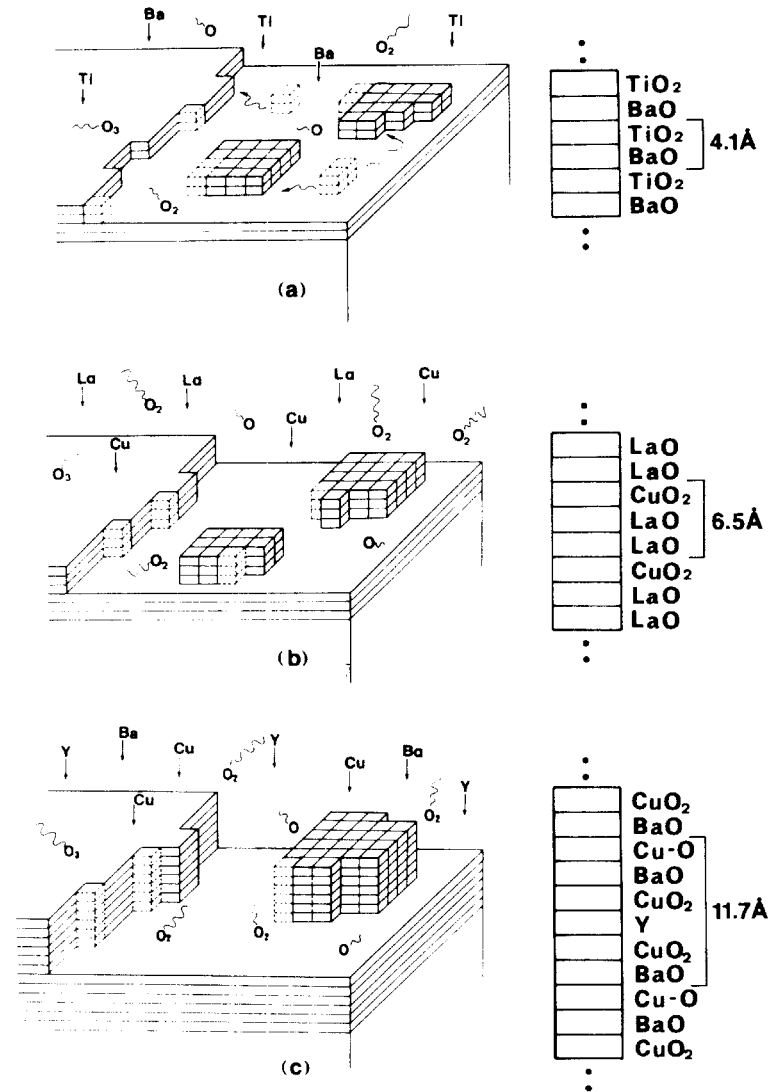
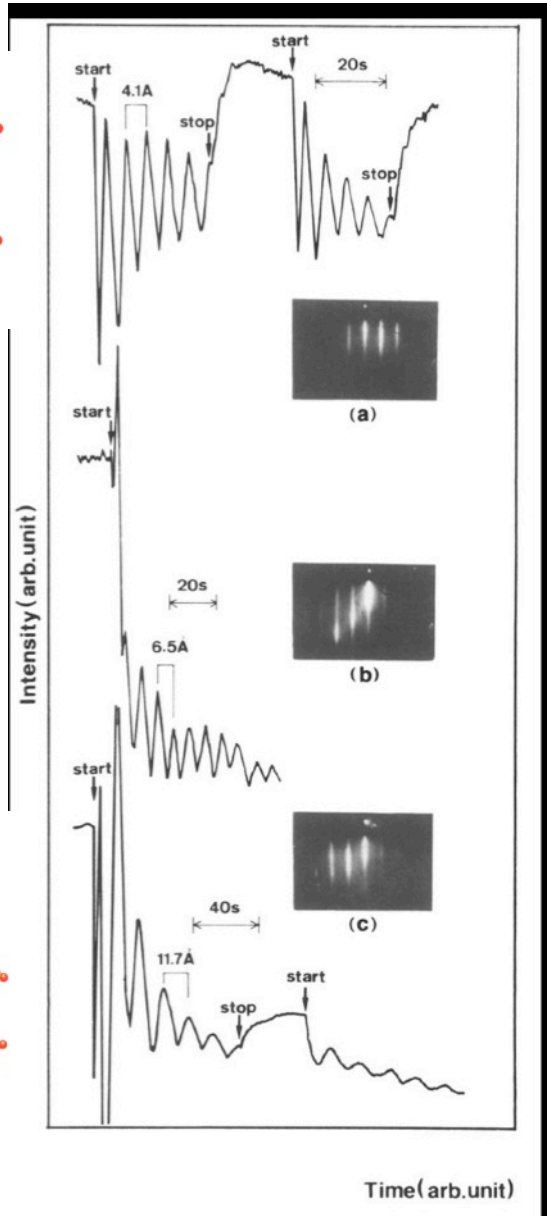
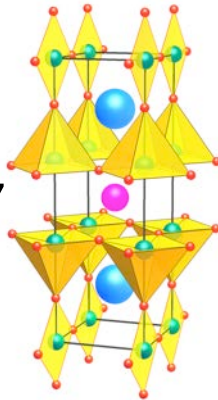
BaTiO_3



La_2CuO_4

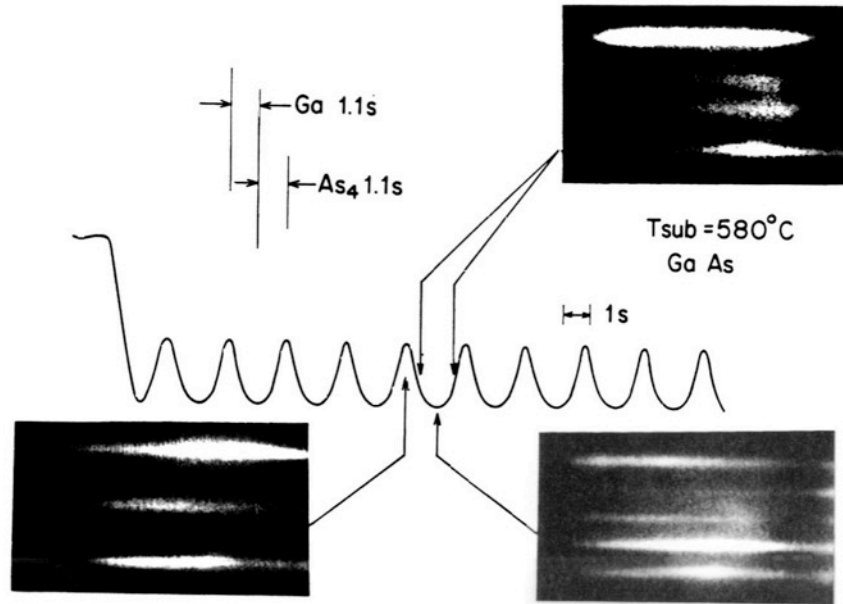


$\text{YBa}_2\text{Cu}_3\text{O}_7$



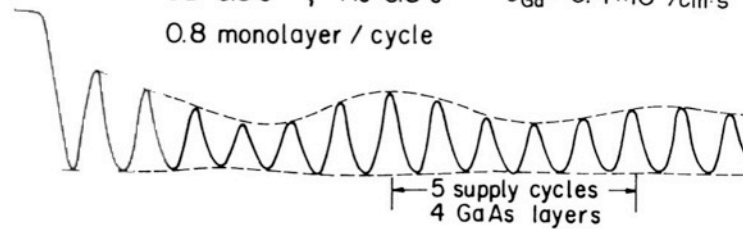
Migration-Enhanced Epitaxy of GaAs and AlGaAs

Yoshiji HORIKOSHI, Minoru KAWASHIMA and Hiroshi YAMAGUCHI

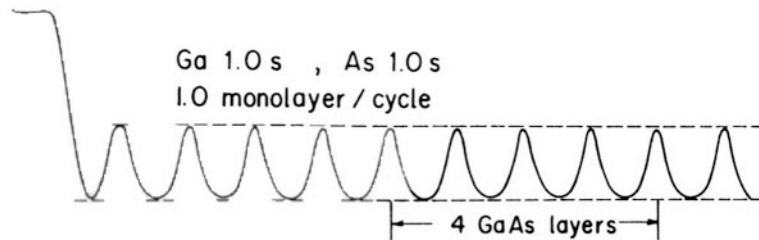


T_s = 580°C

Ga 0.8 s , As 0.8 s $J_{Ga} = 6.4 \times 10^{14} / \text{cm}^2 \cdot \text{s}$
0.8 monolayer / cycle

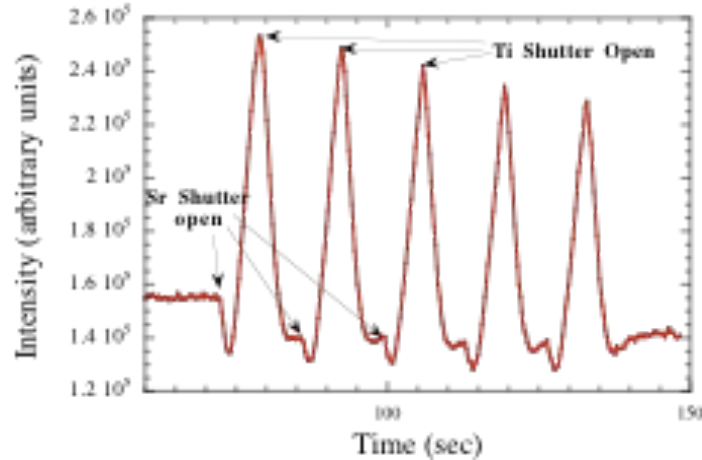


Ga 1.0 s , As 1.0 s
1.0 monolayer / cycle

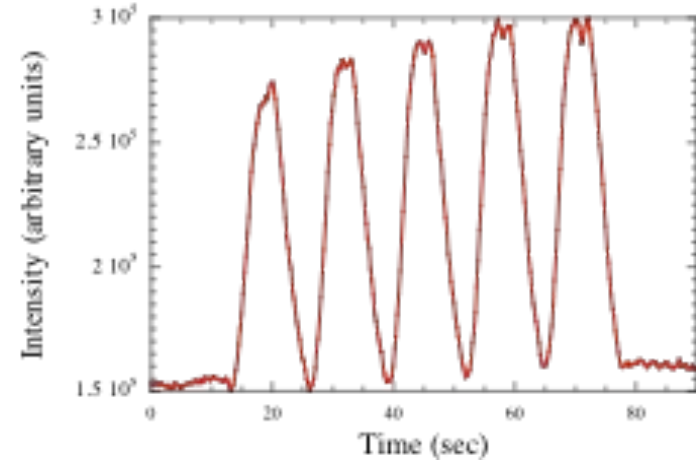


Shuttered RHEED to Get Sr:Ti = 1:1

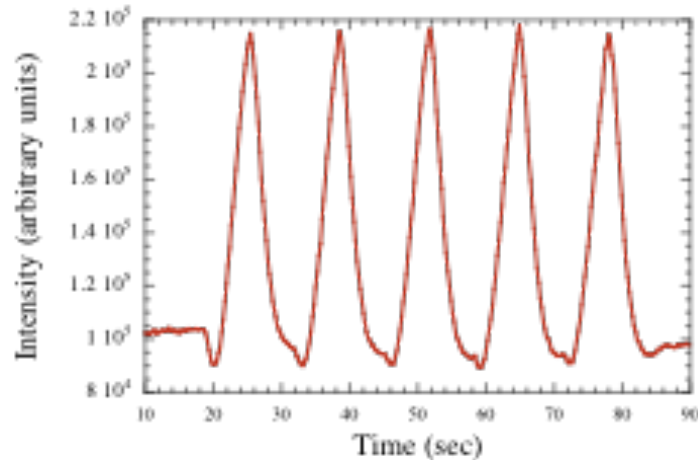
3 % Ti Rich



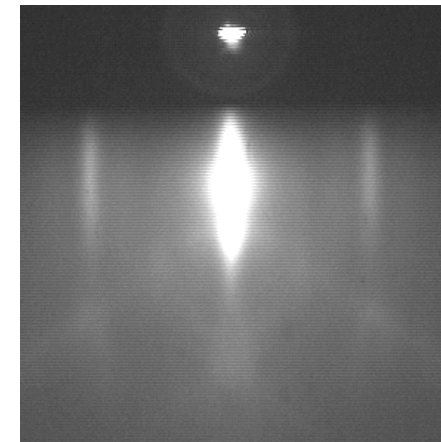
3 % Ti Poor



Stoichiometric

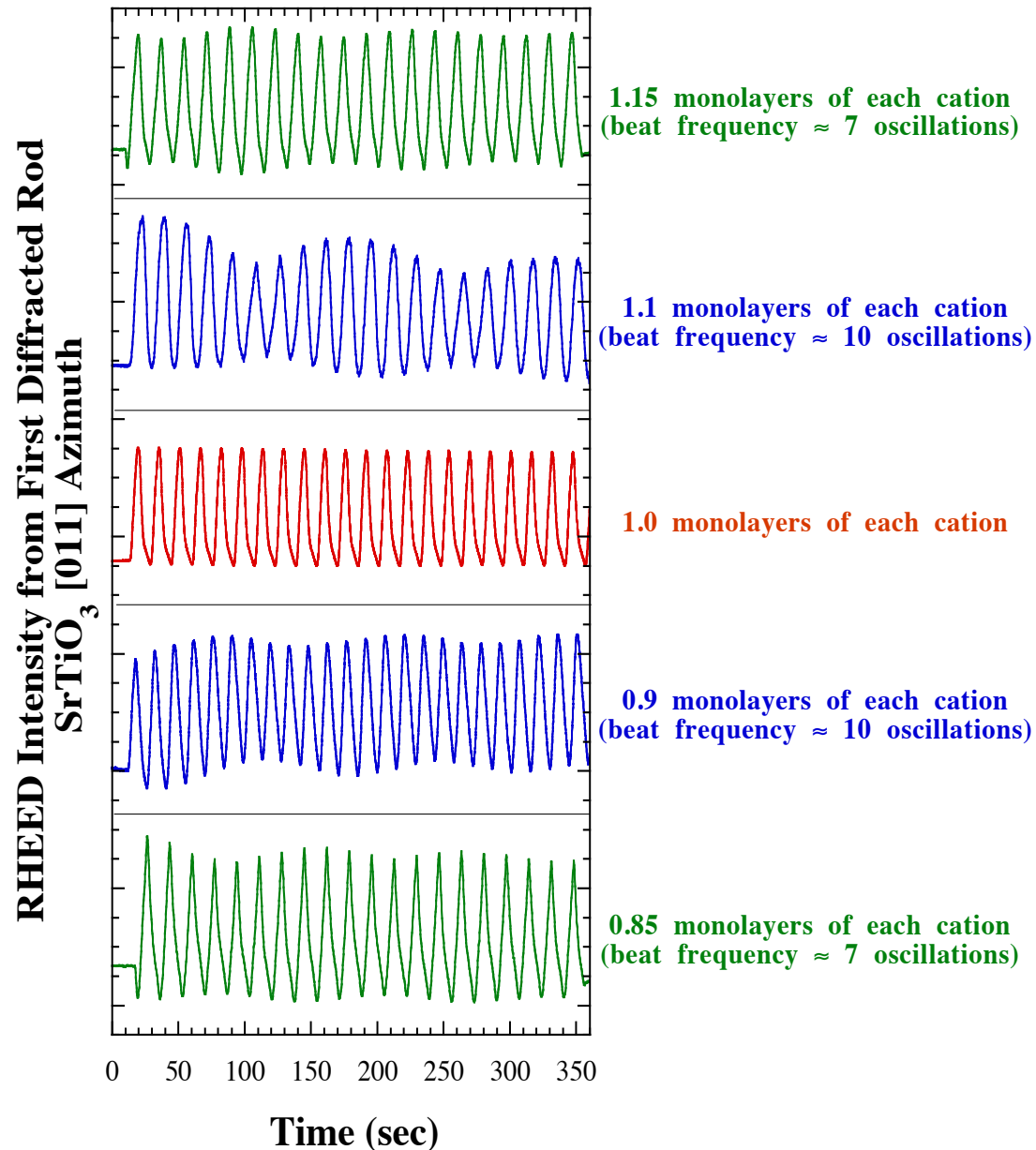


SrTiO₃ [011] Azimuth



Oscillations of the central diffracted rod as the Sr and Ti are deposited in a sequential manner

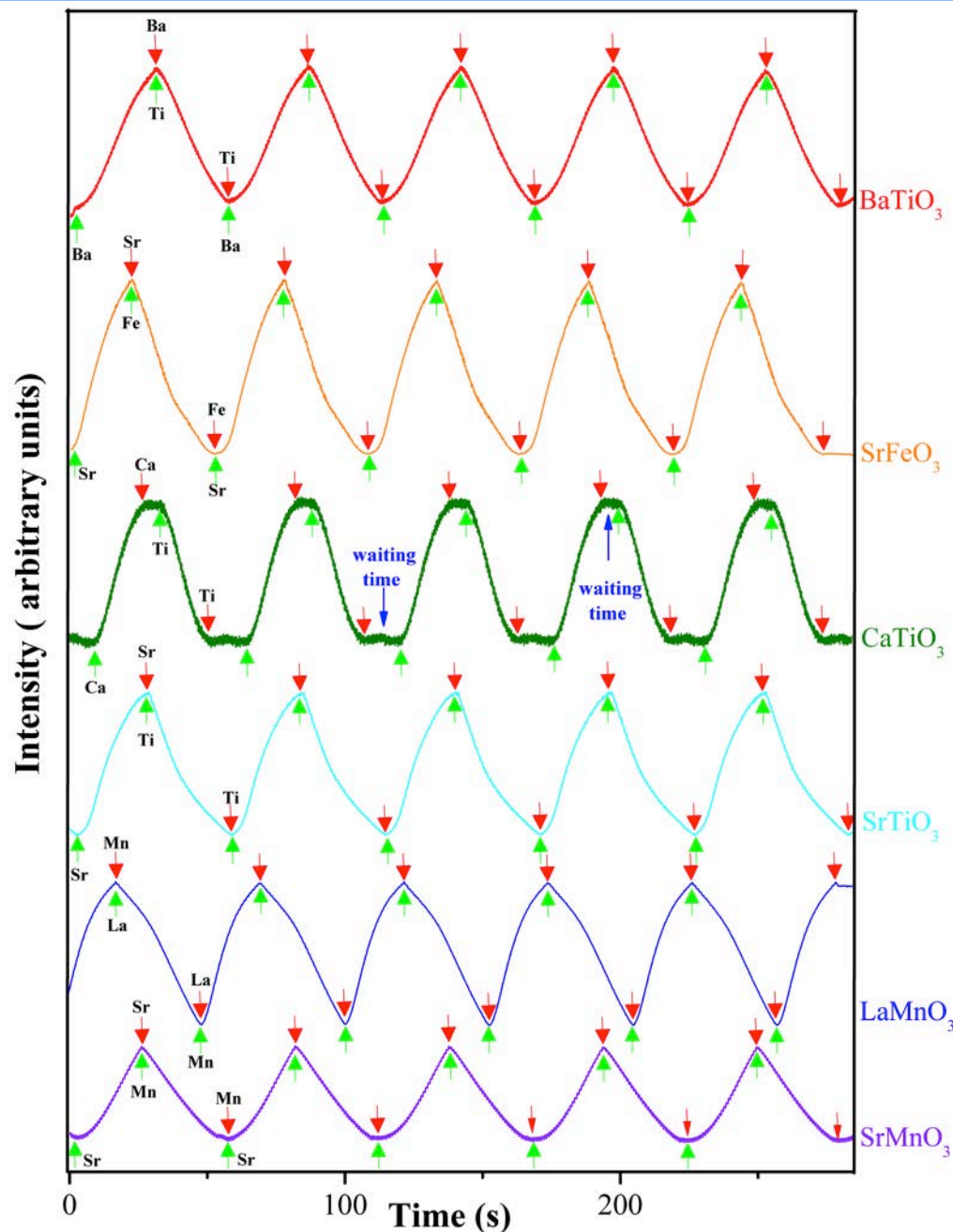
Beat Frequency for Sr:Ti = 1:1 Absolute



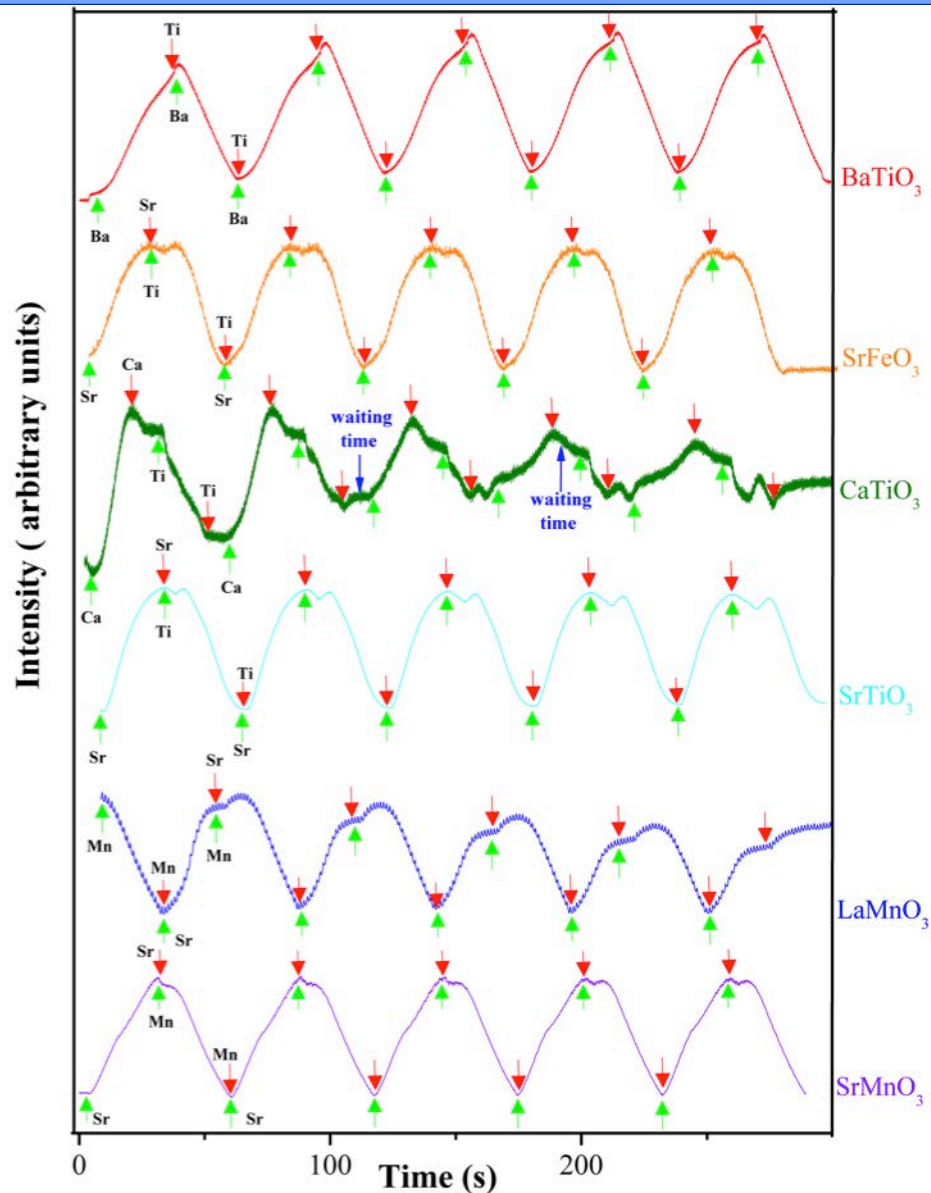
How we do it

- Use Quartz Crystal Microbalance to Get Fluxes Close (~10% accuracy)
- Use Shuttered RHEED Oscillations (analogous to MEE of GaAs)
- Yields Sr:Ti *Relative* Incorporation Ratio (~1% accuracy)
- Yields *Absolute* Monolayer Dose for SrO and TiO₂ (~1% accuracy)
- Works for many Perovskites

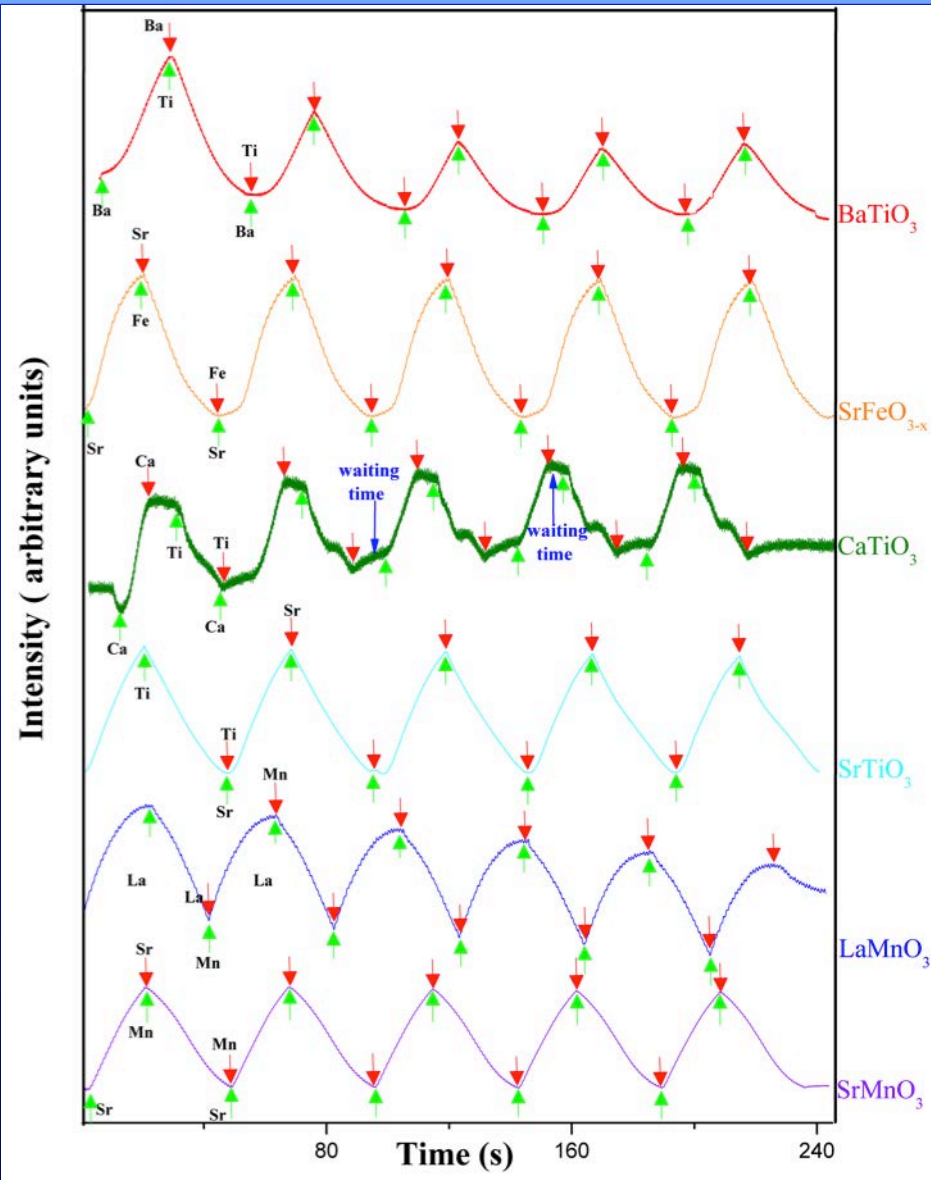
Shuttered RHEED Oscillations



Shuttered RHEED Oscillations



A-Site Rich

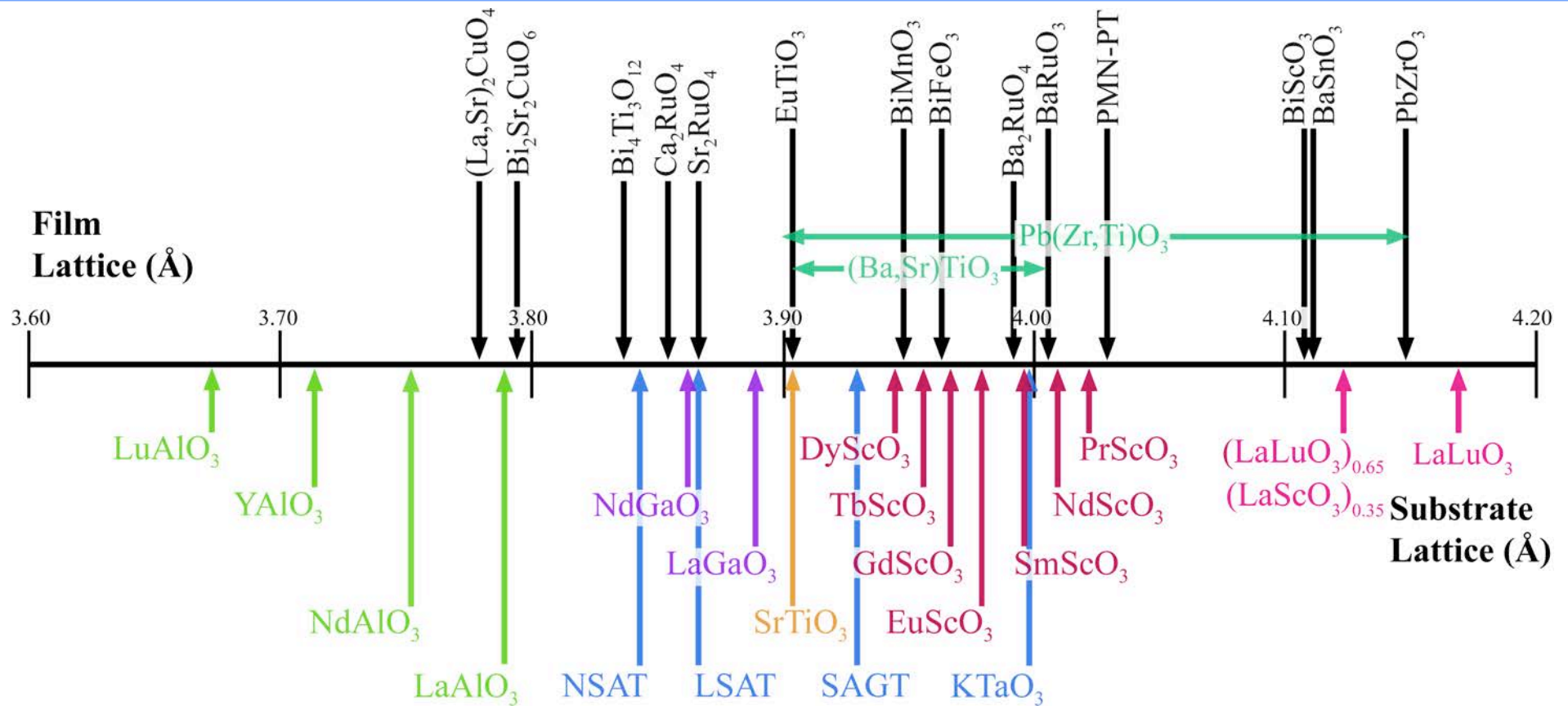


B-Site Rich

Substrates are Key



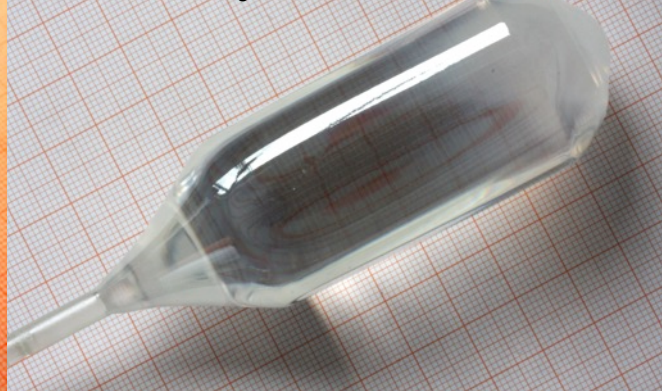
Commercial Perovskite Substrates



[110] DyScO₃, *d* = 32 mm



[110] GdScO₃, *d* = 32 mm



D.G. Schlom, L.Q. Chen, C.J. Fennie,
 V. Gopalan, D.A. Muller, X.Q. Pan,
 R. Ramesh, and R. Uecker,
 “Elastic Strain Engineering
 of Ferroic Oxides,”
MRS Bulletin **39** (2014) 118-130.

Surface Termination Recipes

- **(100) and (111) SrTiO₃**

G. Koster, B.L. Kropman, G.J.H.M. Rijnders, D.H.A. Blank, H. Rogalla, “Quasi-Ideal Strontium Titanate Crystal Surfaces through Formation of Strontium Hydroxide,”

Applied Physics Letters **73** (1998) 2920-2922.

- **(110) REScO₃**

J.E. Kleibeuker, G. Koster, W. Siemons, D. Dubbink, B. Kuiper, J.L. Blok, C-H. Yang, J. Ravichandran, R. Ramesh, J.E. ten Elshof, D.H.A. Blank, and G. Rijnders, “Atomically Defined Rare-Earth Scandate Crystal Surfaces,”

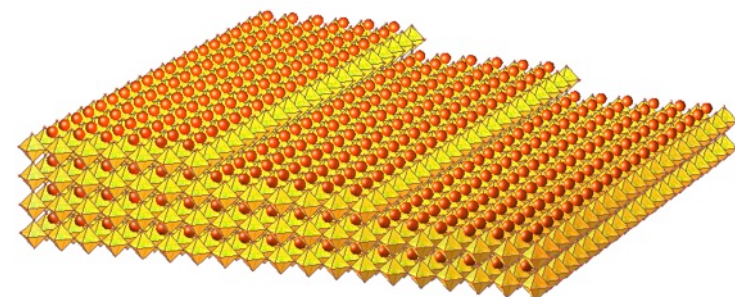
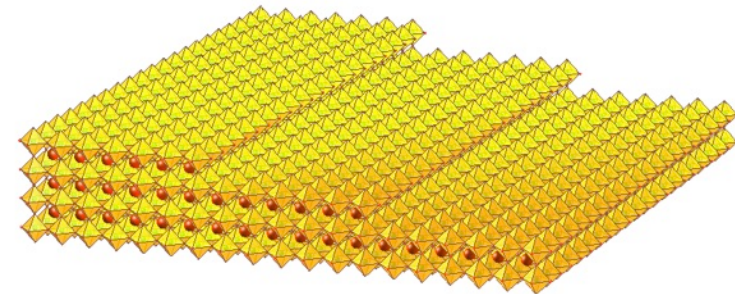
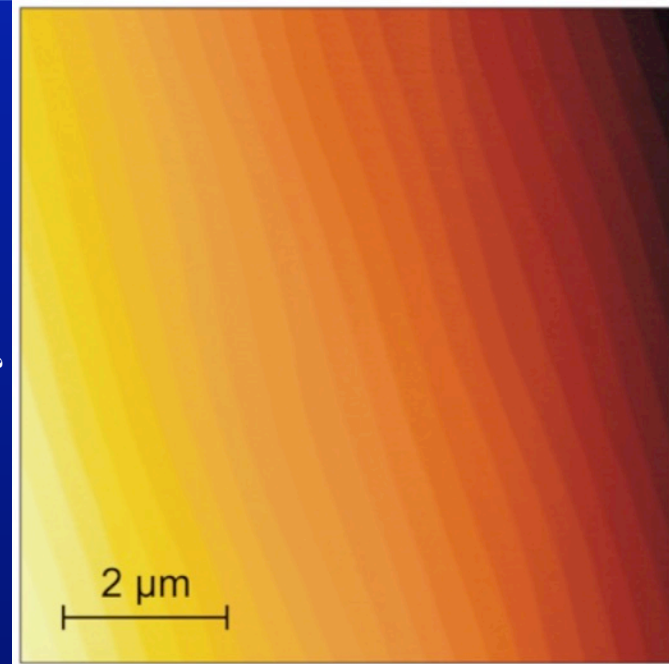
Advanced Materials **20** (2010) 3490-3496.

- **(100)_p and (111)_p LaAlO₃**

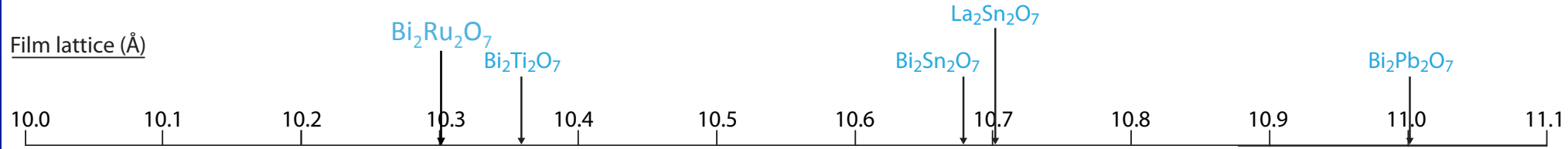
J.L. Blok, X. Wan, G. Koster, D.H.A. Blank, and G. Rijnders, “Epitaxial Oxide Growth on Polar (111) Surfaces,”

Applied Physics Letters **99** (2011) 151917 .

AFM (100) SrTiO₃—Jochen Mannhart

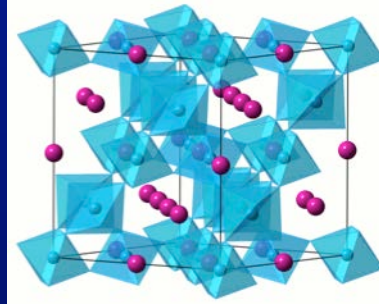


Pyrochlores

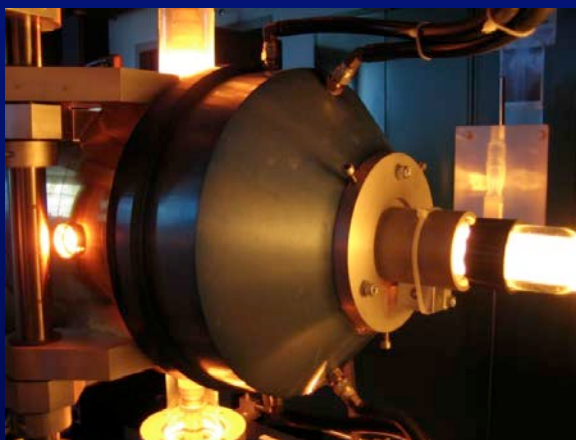
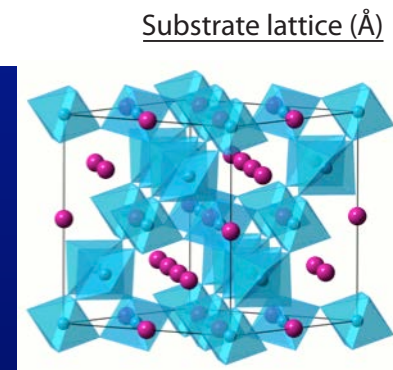
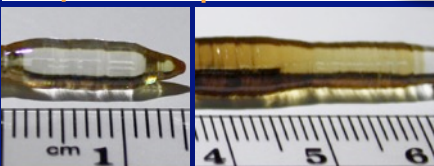
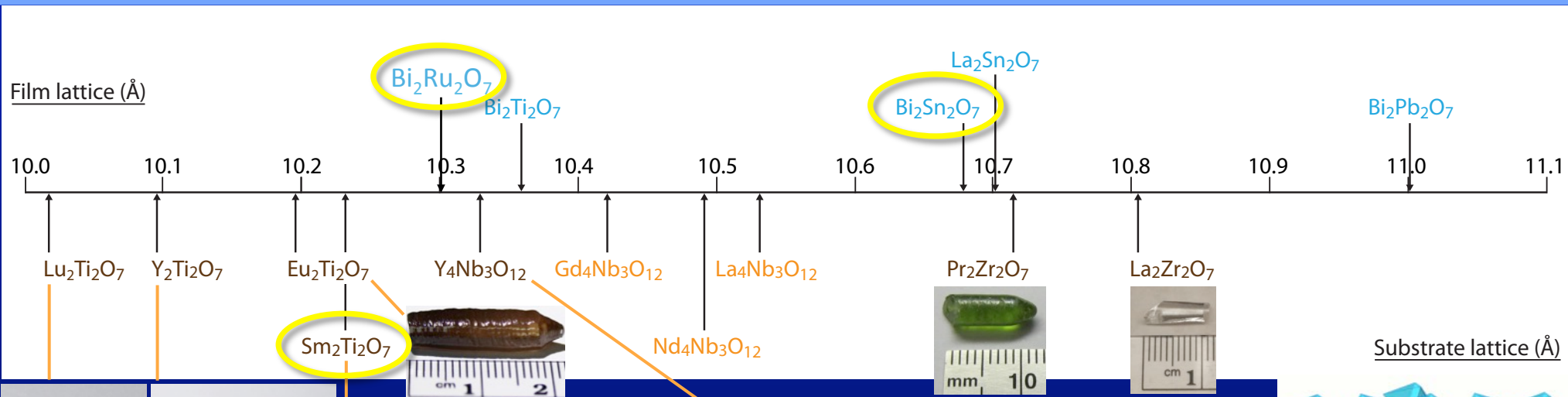


No Commercial Pyrochlore Substrates!

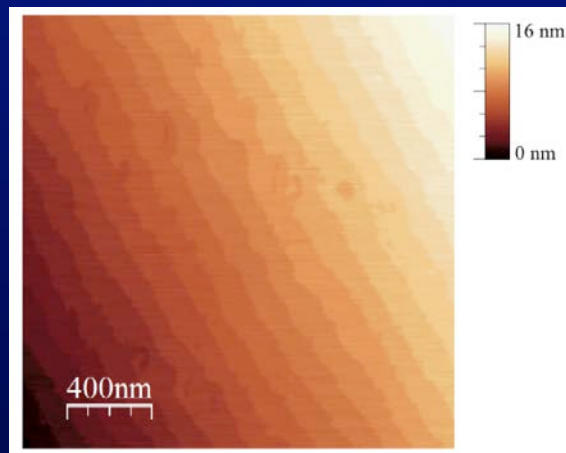
Substrate lattice (Å)



Pyrochlore Substrates



Floating zone furnace (Augsburg)



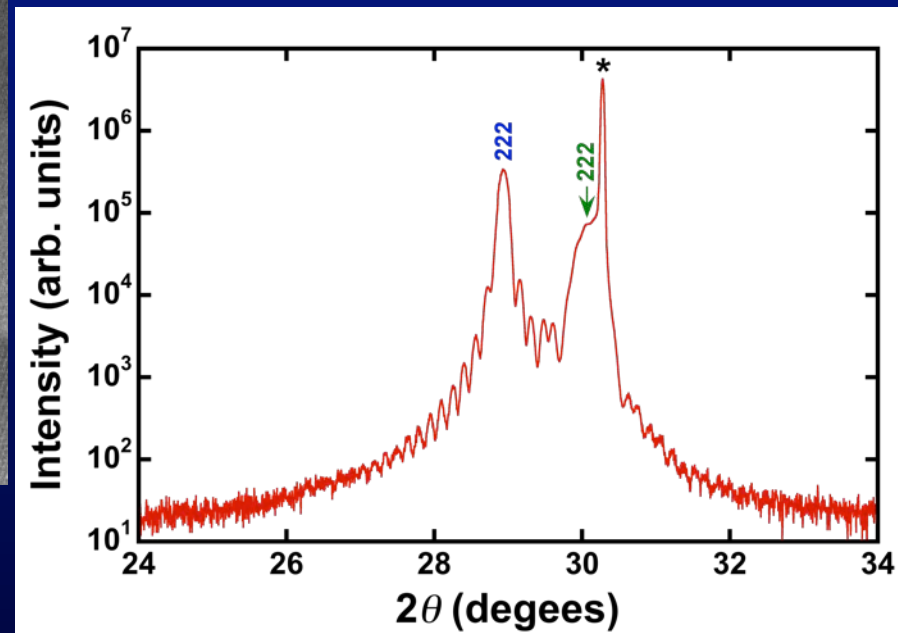
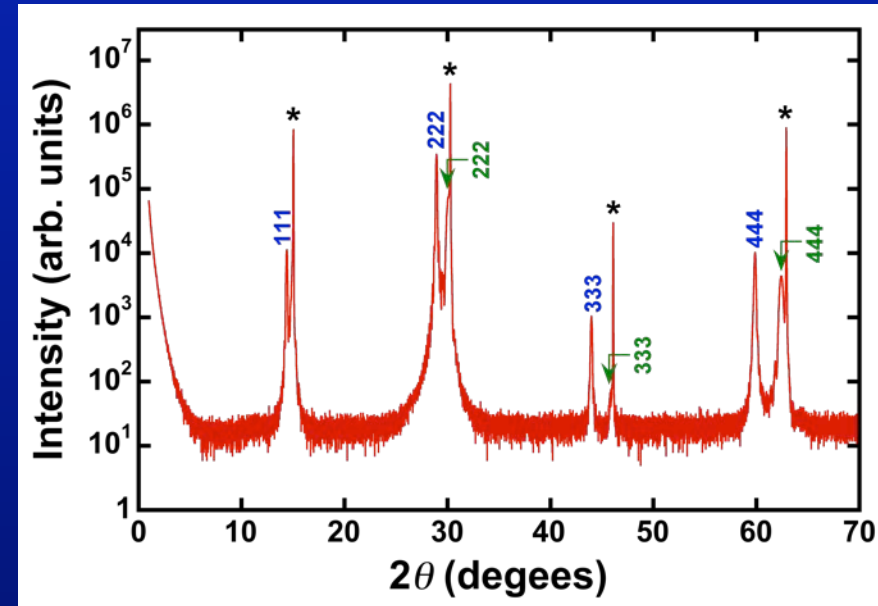
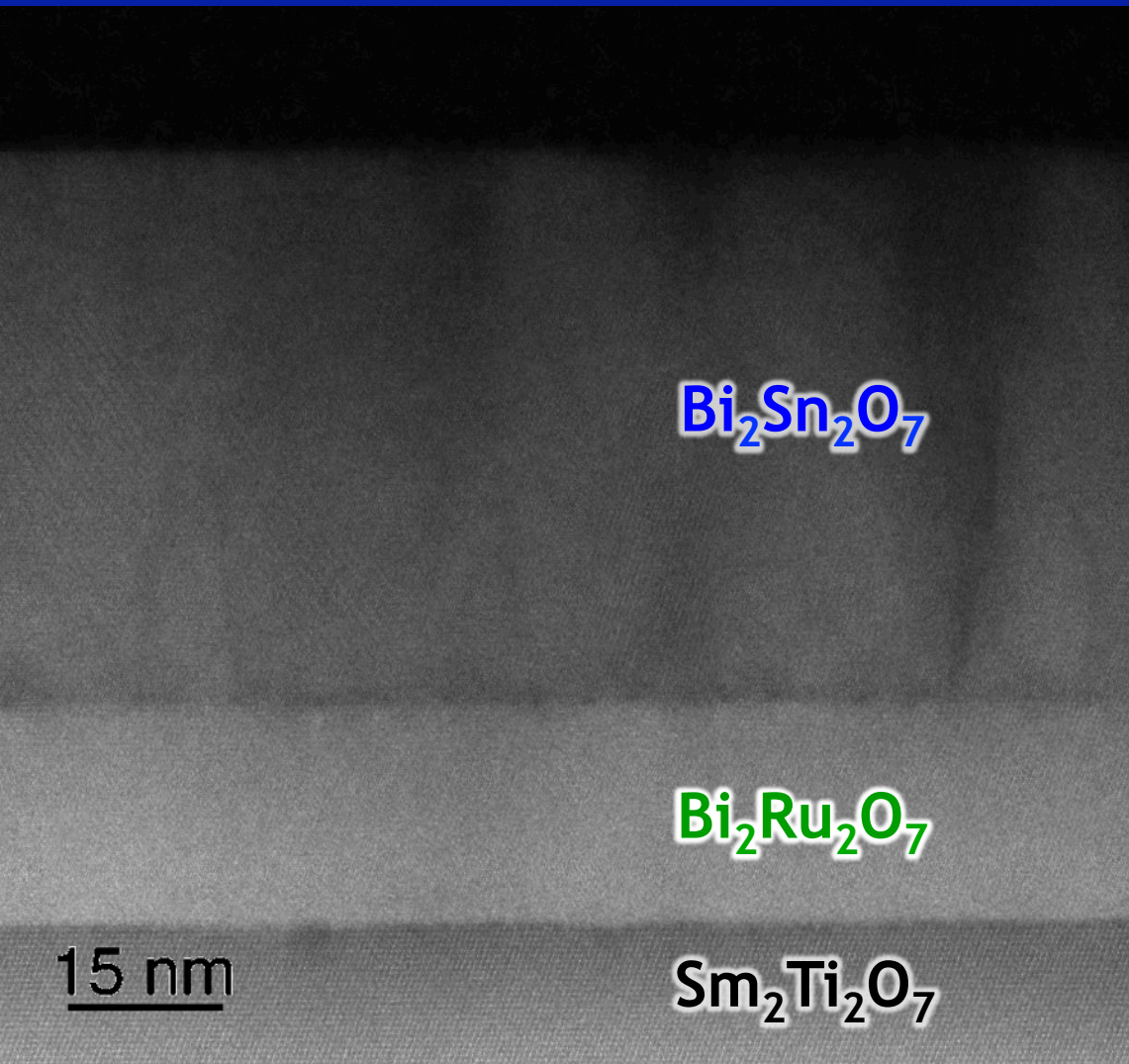
AFM: as-polished (111) $\text{Sm}_2\text{Ti}_2\text{O}_7$ (floating zone)



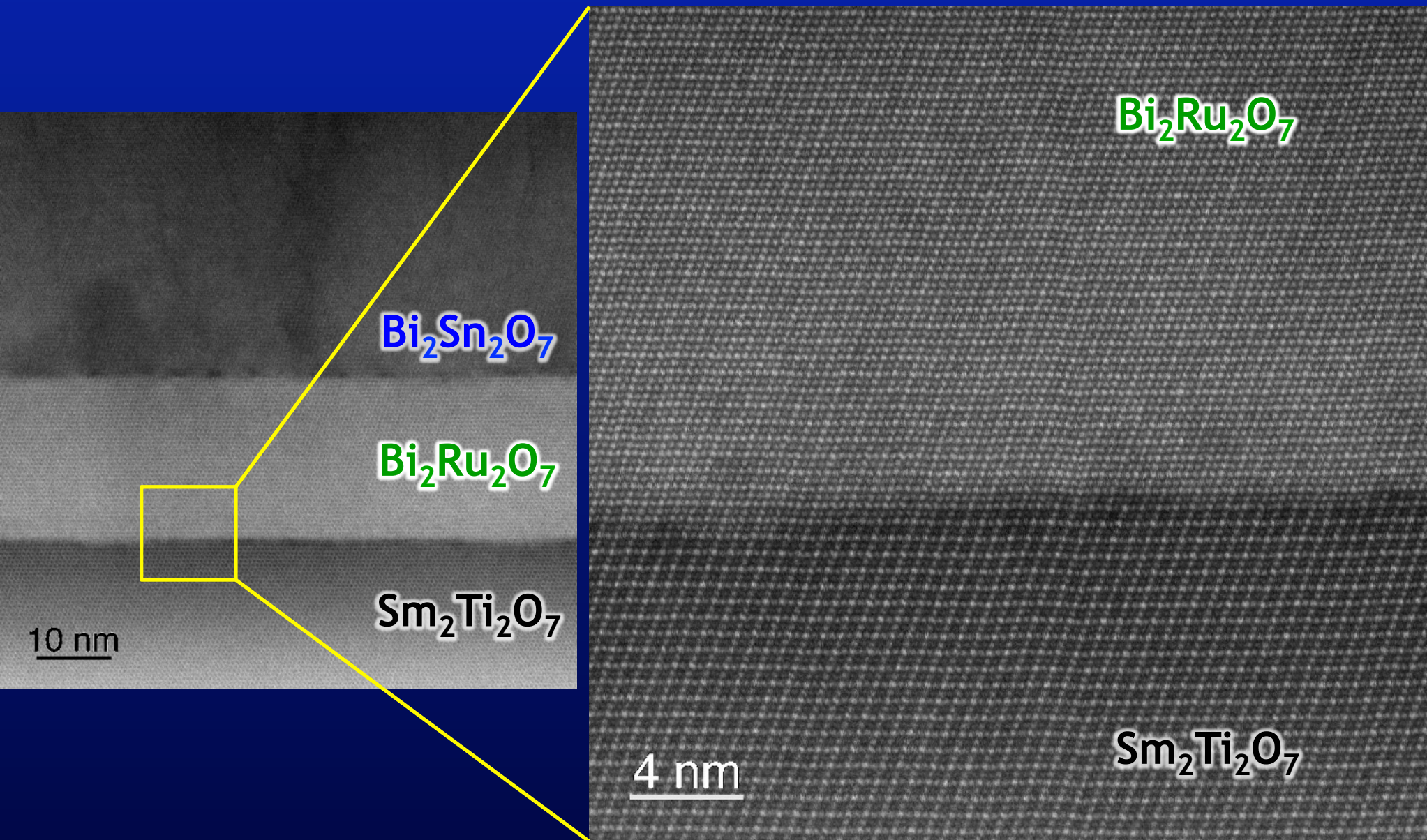
$\text{Sm}_2\text{Ti}_2\text{O}_7$ grown by Czochralski (IKZ, Berlin)

with
Tyrel McQueen
Jochen Mannhart
Reinhard Uecker

MBE of Pyrochlores

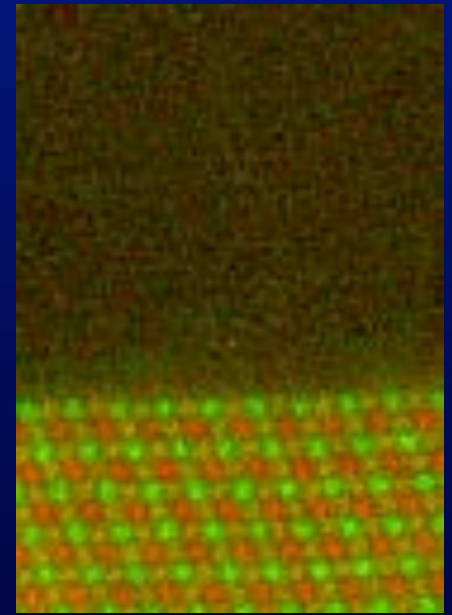
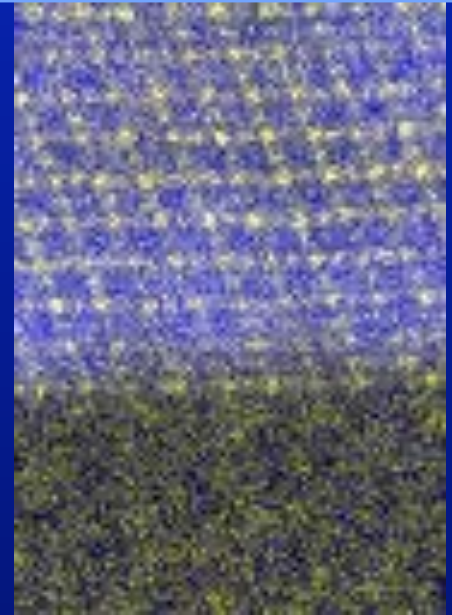


MBE of Pyrochlores

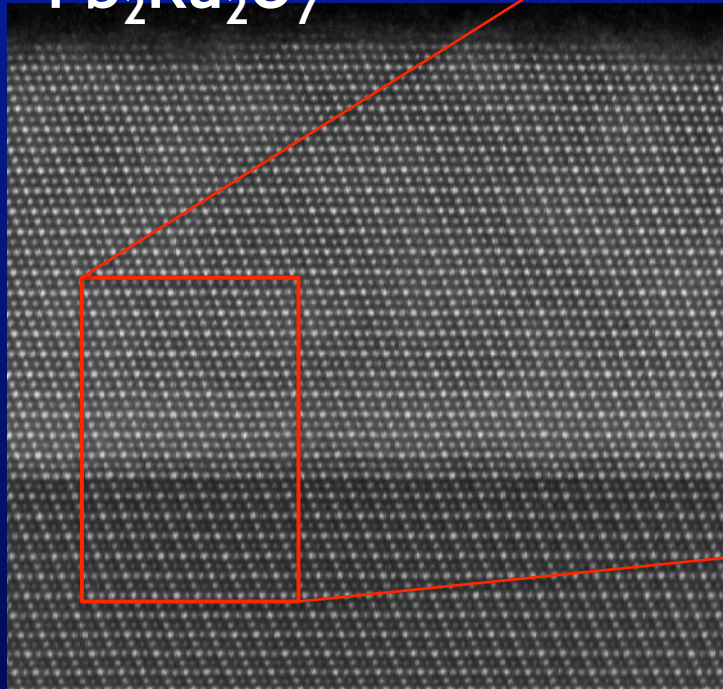


MBE of Pyrochlores

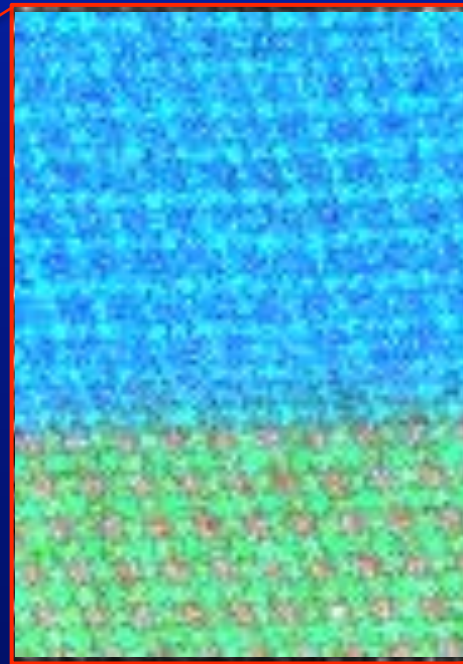
Yellow: Pb, Blue: Ru



$\text{Pb}_2\text{Ru}_2\text{O}_7$



$\text{Sm}_2\text{Ti}_2\text{O}_7$



Red: Ti
Green: Sm
Blue: Ru
Cyan: Pb

Red: Sm, Green: Ti

MBE Summary

Advantages

- Extreme Flexibility
- Independent Growth Parameters
- Compatible with wide range of *in situ* Diagnostics
- Clean
- Gentle
- Precise Layering Control at the Atomic Level

Disadvantages

- Extreme Flexibility (uncontrolled flexibility = chaos!)
 - High Cost
- Long Set-up Time
- MBE (the other meanings...)